Synthesis and Spectroscopic Properties of Diarylethene-Subporphyrinoid Hybrids

Taichi Muto, Nanari Tamiya, Akuto Takagi, Tadashi Mizutani, Didier Bourissou, Gwénaël Rapenne, Mihoko Yamada, Tsuyoshi Kawai

Synthesis and Spectroscopic Properties of Diarylethene-Subporphyrinoid Hybrids

Taichi Muto,[a] Mihoko Yamada,[a] Nanari Tamiya,[b] Akuto Takagi,[b] Tadashi Mizutani,[b] Didier Bourissou,[c] Gwénaël Rapenne,[a][d][e] and Tsuyoshi Kawai*[a][d][f]

[a] Mr. T. Muto, Dr. M. Yamada, Prof. Dr. G. Rapenne, Prof. Dr. T. Kawai*
Division of Materials Science
Nara Institute of Science and Technology
8916-5 Takayama, Ikoma, Nara 630-0192, Japan
tkawai@ms.naist.jp

[b] Ms. N. Tamiya, Dr. A. Takagi, Prof. Dr. T. Mizutani
Department of Applied Chemistry, Graduate School of Science and Engineering
Doshisha University
1-3 Tataramiyakodani, Kyotanabe, Kyoto 610-0321, Japan

[c] Dr. D. Bourissou
Laboratoire Hétérochimie Fondamentale et Appliquée (UMR 5069)
Université de Toulouse (UPS), CNRS
118 route de Narbonne, F-31062 Toulouse, France

[d] Prof. Dr. G. Rapenne, Prof. Dr. T. Kawai
International Collaborative Laboratory for Interfaces, Molecules and Materials
NAIST- Université de Toulouse (UPS)
118 route de Narbonne, 31062 Toulouse Cedex 9, France

[e] Prof. Dr. G. Rapenne
CEMES, Université de Toulouse, CNRS
F-31055 Toulouse, Cedex 4, France

[f] Prof. Dr. T. Kawai
Medilux Research Center
Nara Institute of Science and Technology
8916-5 Takayama, Ikoma, Nara 630-0192, Japan

Abstract: Two novel diarylethene-fused subporphyrinoids were prepared and characterized. A mono diarylethene derivative was obtained *via* a statistical condensation reaction with 2 eq. of 1,2-dicyanobenzene and 1 eq. of thiophene-disubstituted butenedinitrile. The symmetric triply diarylethene-fused subporphyrazine was synthesized *via* a cyclotrimerization reaction of the thiophene-disubstituted butenedinitrile derivative. These compounds were characterized by NMR spectroscopy and high-resolution mass spectrometry. The spectroscopic properties have been measured in hexane and in chloroform. The mono diarylethene-fused-type compound showed photochromism at 580 nm and >700 nm wavelength, accompanied by degradation. According to DFT calculations, photoreactivity likely depends on the contribution of aromatic feature of pyrrole ring bonded to two thiophene rings.

Introduction

After the seminal work of Irie and coworkers, photochromic diarylethene (DAE) has garnered significant attention among organic chemists and photochemists. Its appeal stems from both fundamental perspectives, such as its photochemical peri-cyclization reactivity, and its potential for chemical hybridization with a wide array of substances.[1] Due to its unique properties, like high durability, high photochemical reactivity even in single crystals,[2] and thermal stability of both isomers, diarylethenes have been studied as promising candidates for future optical recording and photo-responsive molecular switches. Their photochromic reactions enable the reversible modulation of various molecular properties when combined with appropriate functional units. For instance, extensive research has focused on efficient fluorescence photoswitching through the incorporation of fluorescent units in their side chains.[3] Various functional units have been also introduced onto the central bridging ethene unit.[4] The DAE hybridized with phthalocyanine showed photochromic cyclization and cycloreversion under visible light irradiation of longer than 700 nm in wavelength.[5] Recently, we have also reported DAE fused on the curved aromatic corannulene, a central aromatic curved unit with a C_5 symmetry.[6] The significantly high photosensitivity obtained stimulated us to explore the subphthalocyanine as a new curved aromatic scaffold, which consists of three iminoisoindol subunits embedded in a C_3-symmetric structure. Since the first report by Meller and Osako,[7] the subphthalocyanine scaffold has attracted significant attention because of its curved 14π electron

conjugated core and unique electronic and fluorescence properties.[8-9] Despite DAE has been introduced to the axial position of subphthalocyanine for fluorescence photoswitching capability,[10] it is still challenging to explore the potentiality of subphthalocyanine with peripherally fused DAE fragments. Here, we report the synthesis and the spectroscopic properties of the DAE-fused subphthalocyanine, **SubPc-DE$_1$** and a triply DAE-fused subporphyrazine analogue, **SubPz-DE$_3$** (Scheme 1). Very recently, a similar subporphyrazine derivative **SubPz-DE$_1$-^{n}Pr** (Scheme S1) has been independently investigated by E. Cañizares-Espada *et al.,* indicating reversible photochromic feature.[11] We here also attempt to compare these substances based on quantum chemical calculations.

Results and Discussion

Synthesis and Characterization

The dissymmetric subphthalocyanine **SubPc-DE$_1$** bearing one fused diarylethene was synthesized following a statistical condensation reaction. Two equivalents of 1,2-dicyanobenzene were reacted in the presence of boron trichloride with one equivalent of (2*Z*)-2,3-bis(2,5-dimethyl-3-thienyl)-2-butenedinitrile[12] followed by the axial ligand exchange reaction with phenol (Scheme 1). After purification by column chromatography, **SubPc-DE$_1$** was obtained in pure form as a purple solid in 0.7% yield. This low yield is not due to the statistical conditions of the reaction which limit the yield to 44%,[13] but mainly by the low stability of the dithienylethene derivative in these conditions. After the first step, a dark brown tar-like material was observed corresponding to the decomposed dithienylethene at high temperature in presence of BCl_3. This reaction condition is usually performed in synthesis of subporphyrazine analogue.[8] Reaction at a lower temperature by using BBr_3[14] instead of BCl_3 gave no positive result. However, even with a low yield, the quantity of pure molecule was enough to study its spectroscopic properties

High-resolution mass spectrometry (MALDI-TOF) of the obtained compound showed a molecular ion peak at *m/z* = 658.1776 (calcd for $BC_{38}H_{27}N_6OS_2$ = 658.1782 [SubPc-DE$_1$]$^+$) (Figure S1). In the ^{1}H NMR spectrum (Figure S2), two singlets at 2.47 and 2.38 ppm were assigned to the two methyl groups of the thiophene rings. Also, a singlet at 6.69 ppm was assigned to the proton at the 4-position of the thiophene ring. The integration of the ^{1}H NMR signals was also particularly informative with the expected 2:1 ratio between the phthalocyanine subunits compared to the dithienyl fragment. ^{1}H-^{1}H COSY further helped us to assign two singlets at 2.47 and 2.38 ppm to the methyl substituents at 5- and 2-position of the thienyl rings, respectively (Figure S3) which was confirmed by the ^{1}H-^{1}H NOESY spectrum (Figure S4). This correlation signal also confirmed the existence of DAE unit of **SubPc-DE$_1$** in the anti-parallel conformation which is necessary to allow the photocyclization to occur. Three signals at 6.79, 6.64, and 5.45 ppm were assigned as the protons of the axial phenoxy ligand at the *meta*-, *para*-, and *ortho*-position respectively. Their high field character is due to the influence of the subphthalocyanine's shielding cone.[15] The ^{13}C NMR spectrum exhibits twenty peaks, which is consistent with the chemical structure of **SubPc-DE$_1$** (Figure S5).

As shown on Scheme 1, the synthesis of the symmetric subporphyrazine analogue with three diarylethene units **SubPz-DE$_3$** was similarly synthesized in a quite low yield of 0.2% following the methodology described by Torres *et al.*[16] in presence of boron trichloride. Although we tested other reaction conditions, the yield never exceeded 0.2%. HR-MS (MALDI-TOF) of the obtained product showed a molecular ion peak at *m/z* 998.2228 corresponding to the expected molecule (Figure S6). The ^{1}H NMR spectrum (Figure S7) exhibit three singlets at 6.76, 2.44, and 2.37 ppm which were assigned to the 4-position proton, the 5-methyl and the 2-methyl of the thiophene rings. The three signals at 6.83, 6.66, and 5.44 ppm were also attributed to the *meta*-, *para*-, and *ortho*-protons of the boron-coordinated phenoxy ligand

with the expected 2:1:2 ratio. The similar high-field chemical shifts of phenyl protons demonstrate that the ring current effect is almost the same in the two porphyrinoids.

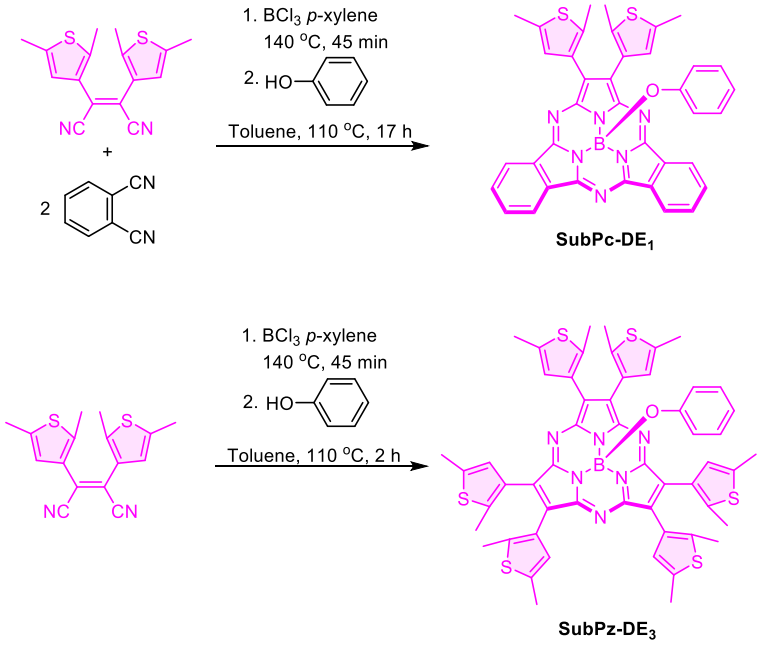

Scheme 1. Synthesis of **SubPc-DE$_1$** and **SubPz-DE$_3$**.

With the aim to clarify the effect of steric hindrance on the lateral thiophene fragments, we also tried to synthesize the subphthalocyanine analog **SubPc-DE$_1$-Me** bearing an additional methyl group at the 4-position of the thiophene rings (Scheme S2). Unfortunately, the desired compound was not obtained, which revealed that the higher steric effect of the thiophene ring prevent the boron-templated cyclotrimerization reaction to occur.[17]

Optical properties

The UV-visible absorption spectrum of **SubPc-DE$_1$** in hexane exhibits a Q-band at 570 nm and a Soret band at 306 nm (Figure 1a). After excitation, **SubPc-DE$_1$** also exhibits fluorescence at 580 nm, which is similar to those of conventional subphthalocyanine analogues.[14] In a polar solvent like chloroform, **SubPc-DE$_1$** exhibits a Q-band at 575 nm, a Soret band at 309 nm, and fluorescence at 595 nm (Figure S8). The fluorescence quantum yield was estimated to be 5% in chloroform as well as in hexane.

SubPz-DE$_3$ shows a Q-band at 556 nm and a Soret band at 300 nm in chloroform (Figure S9). The π-conjugation of **SubPz-DE$_3$** is less extended than **SubPc-DE$_1$** with two fused benzene rings, resulting in a shift of the Q-band and the Soret band towards shorter wavelengths. **SubPz-DE$_3$** also exhibits absorption at 440 nm, which can be assigned to the n→π* transition from the peripheral thiophene rings into the π macrocyclic orbital, considering similar absorption at 444 nm of hexathioalkyl-substituted subporphyrazine due to n→π*.[18]

Photochromism

SubPc-DE$_1$ exhibits photochromic spectral change in hexane (Figure 1a and 1b). Upon irradiation with 580 nm light, the Q-band at 570 nm gradually decreased and a new absorption band around 700 nm appeared. This new absorption was faded by illumination of light, l > 700

nm with recovering of the Q-band. As described below, this new absorption band at 700 nm was ascribed to the ring-closed form by TD-DFT calculations (Figure S13). The interconversion between the open and closed form could be repeated at least 5 times (Figure 1c).

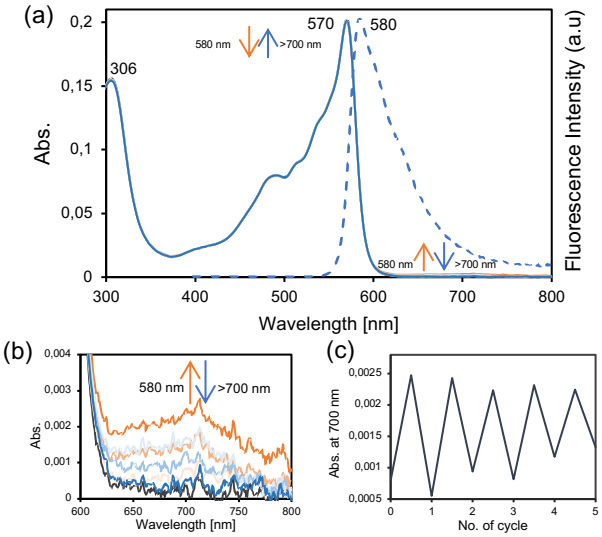

Figure 1. (a) UV-vis absorption spectral change and fluorescence spectrum (excitation wavelength: 333 nm) of **SubPc-DE$_1$** in hexane (2×10^{-5} M). Irradiation with 580 nm light until the photostationary state and following >700 nm light irradiation. (b) The enlarged view of (a) around 600-800 nm. (c) Photoswitching performance of **SubPc-DE$_1$** in hexane monitored by UV-vis spectroscopy at 700 nm (2×10^{-5} M, Irradiation with 580 nm light until the photostationary state and following >700 nm light irradiation).

Similar spectral change was also reported for the **SubPz-DE$_1$-^{n}Pr**.[11] In the present study, unfortunately, the degree of absorbance change at 700 nm became smaller with repetitive cycles, indicating the photochromism is accompanied with some degradation (see also Figure S10). Since we observe a decrease of 1.2% between the maximum peaks from the first to the fifth cycle, we can evaluate average decomposition to be about 0.2% per cycle but the tendency is not constant with a higher value in the first cycles. A chloroform solution of **SubPc-DE$_1$** also showed photochromism with 580 nm and >700 nm light, but the decomposition rate in chloroform is 2.3% per cycle, suggesting **SubPc-DE$_1$** decomposes more easily in chloroform (Figure S11).

This observed absorption change appears relatively small in comparison with the large absorbance of the Q-band. While direct comparison is challenging due to variations in solvent and other experimental conditions, such as the different solvent utilized in this study compared to that in the previously reported paper,[11] a lower photoreactivity of **SubPc-DE$_1$** is expected.

The photochemical reactions of **SubPc-DE$_1$** were also studied by ^{1}H NMR (Figure 2).[19] Different signals were observed in the ^{1}H NMR spectra after irradiation in the 510-590 nm range and mostly returned to the original spectrum by irradiation with > 700 nm light. The new doublet observed at 5.8 ppm was assigned to the *ortho*-proton of the axial phenoxy group which was shifted from 5.4 to 5.8 ppm during the photocyclization, suggesting the suppression of the diatropic ring current in the closed form. The conversion ratio from the open to the closed form was estimated to be about 5% based on the integration value of the *ortho*-proton of the axial phenoxy group between the open and closed form. We also observed an irreversible appearance of new peaks around 4 ppm and 7.4-7.6 ppm after irradiation at > 700 nm, suggesting decomposition of **SubPc-DE$_1$**. This decomposition suggests a low fatigue-

resistant property for **SubPc-DE$_1$**. However, **SubPz-DE$_3$** showed a more complicated behavior with the Q-band gradually decreasing upon irradiation with > 560 nm light in chloroform, and the appearance of a new absorption band around 700 nm which showed no obvious reversibility(Figure S13). Since **SubPz-DE$_1$-^{n}Pr** has been reported to display high photochemical conversion yield without marked photodecomposition, we attempted to compare these molecules with the support of DFT calculations.

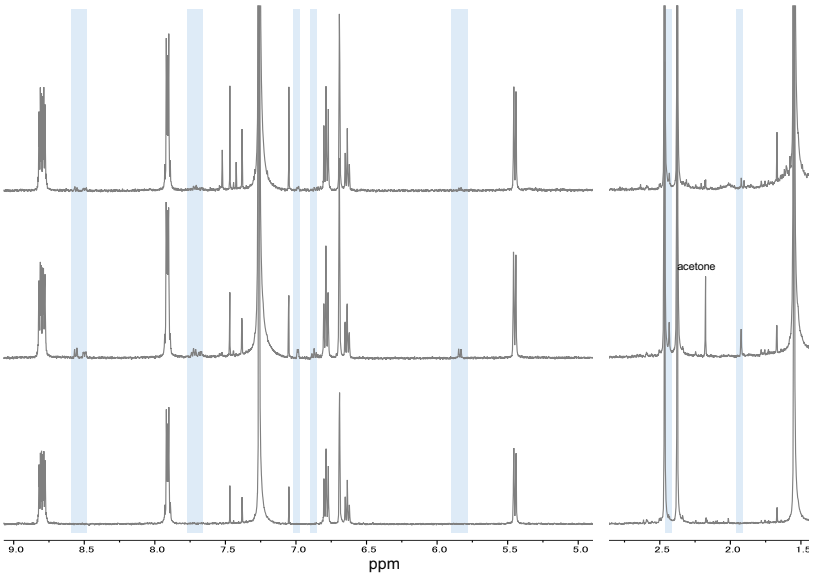

Figure 2. ^{1}H NMR spectra (500 MHz, $CDCl_3$, 298 K) of (a) **SubPc-DE$_1$** and (b) after 510-590 nm light irradiation and (c) after following > 700 nm light irradiation. The new peaks obtained after irradiation are highlighted in light blue.

DFT calculation

Quantum chemical calculation was carried out based on DFT and TD-DFT procedure at B3LYP/6-31+G(d,p) level for **SubPc-DE$_1$**, **SubPz-DE$_3$**, and the previously reported **SubPz-DE$_1$-^{n}Pr** as a reference. Local aromatic feature was characterized with Nucleus-Independent Chemical Shifts (0), NICS(0).[20]

As shown in Figure 3, the calculation for **SubPc-DE$_1$** and **SubPz-DE$_3$** successfully revealed typical bowl-shaped structures of subphthalocyanine unit with axial coordination of phenoxy group. The thiophene rings at the DAE unit are twisted toward the central pyrrole ring. The twisting feature of each couple of thiophene units form the quasi C_2-symmetric hexatriene structure as the anti-parallel conformation. The distance between the reactive carbon atoms is 3.64 Å and 3.63 Å for **SubPc-DE$_1$** and **SubPz-DE$_3$**, respectively, which are suitable for photochemical peri-cyclization reaction.[21] These structures are rationally supported by the NMR spectra.

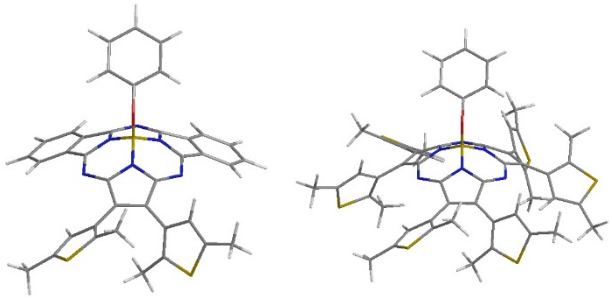

Figure 3. Structure optimized by DFT calculation (B3LYP/6-31+G(d,p)) of **SubPc-DE$_1$** (left) and **SubPz-DE$_3$** (right).

The TD-DFT calculations carried out on **SubPc-DE$_1$** (Figure S14a) showed a characteristic transition band at 500 nm, which is consistent with the observed Q-band of the subphthalocyanine unit. The closed form of **SubPc-DE$_1$** was also evaluated to show a typical absorption band at a little longer wavelength with a long tail (Figure S14b), which again roughly reproduce the observed colored state. The $S_0 \rightarrow S_1$ transition of **SubPc-DE$_1$** is composed of transitions from the HOMO to the LUMO and the LUMO + 1, and the HOMO - 1 to the LUMO (as shown in the table of Figure S15). Similar results were essentially obtained for **SubPz-DE$_3$** and **SubPz-DE$_1$-^{n}Pr**.

The NICS(0) values of three pyrrole rings of **SubPc-DE$_1$** were calculated as -8.15, -4.86, and -4.88 for the open form, but 2.14, -6.48, and -6.46 for the closed form (Figure S16). The pyrrole ring next to the two thiophene rings has a higher aromaticity than the other pyrrole rings fused with the benzene rings. Under the assumption of simple bond-alteration of 14p-electron systems[22] (Figure S18), the pyrrole rings on the dibenzo-subporphyrazine structure should be illustrated as the aromatic or quinoid types (Scheme 2). The lower aromaticity of the two pyrrole rings next to the benzene rings suggests a major contribution of the quinoid form, while the pyrrole ring involved in the DAE local structure could be more aromatic.

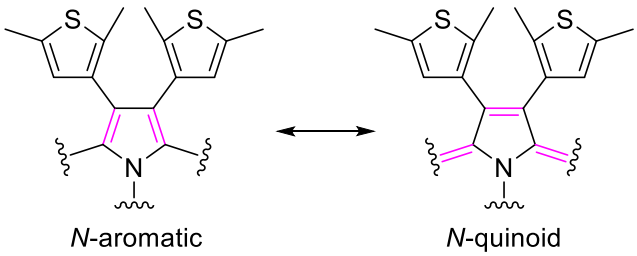

Scheme 2. Two different resonance forms of the pyrrole ring in **SubPc-DE$_1$** and **SubPc-DE$_1$-^{n}Pr** with the involved π-electrons shown in red.

We also evaluated NICS(0) values for **SubPz-DE$_1$-^{n}Pr** to be -7.73, -8.29, and -8.23 (Figure S17). These results imply that the pyrrole rings fused with benzene ring are less aromatic. On the other hand, the DAE subunit fused with the dibenzosubporphyrazine fragment could be less suitable for the photochemical cyclization of **SubPc-DE$_1$**. Energy difference between the open and the closed form was 3.7 kJ/mol higher in **SubPc-DE$_1$** (69.07 kJ/mol) than **SubPz-DE$_1$-^{n}Pr** (65.37 kJ/moll), which seems not so significant as the origin of their difference in the photochemical properties.

We also studied the spatial distribution of the HOMO and LUMO of **SubPc-DE$_1$**. As illustrated in Figure 4, they both showed similar distribution around the central DAE subunit and possibly characterized as quasi anti-σ-symmetry, which are not suitable for classic

understanding of 6p-photocyclization reaction. It is worth noting that HOMO-1 is more localized on the DAE part and suitable for the photocyclization with quasi s-symmetry (Figure S15).

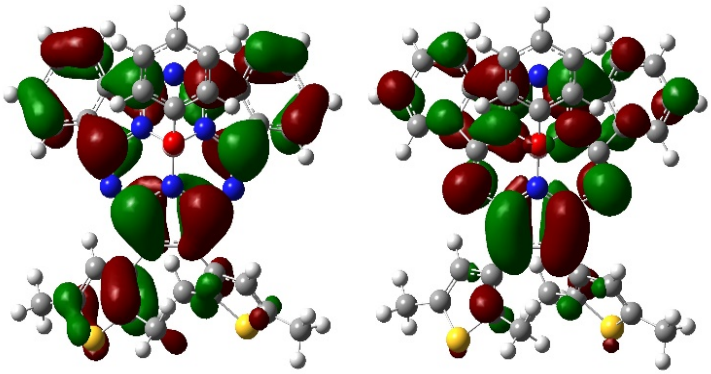

Figure 4. HOMO (left) and LUMO (right) of **SubPc-DE$_1$**. DFT calculation level: B3LYP/6-31+G(d,p)

Similarly, **SubPz-DE$_1$-^{n}Pr** also displays a quasi anti s-symmetric HOMO and LUMO dispersion (Figure S20), as DAE proceeds in photocyclization reaction with symmetric HOMO and asymmetric LUMO in a conrotatory process. The photocyclization in a present system could also occur *via* an unusual manner. Recently, Fukaminato *et al.* have reported an efficient photocyclization of DAE through the triplet excited state[23] and previously cation radical mechanism[24] has also been also demonstrated.

Conclusion

In conclusion, we here synthesized new subphthalocyanine-fused DAEs, the dissymmetric diarylethene-fused subphthalocyanine **SubPc-DE$_1$** *via* a statistical condensation reaction and the symmetric triply diarylethene-fused subporphyrazine **SubPz-DE$_3$** *via* a cyclotrimerization reaction of the thiophene-disubstituted butenedinitrile derivative. These compounds exhibit similar Q-band and Soret band in their absorption spectra. **SubPc-DE$_1$** showed partial photocyclization under irradiation at 580 nm and the cycloreversion occurred with >700 nm light in hexane and in chloroform. Evaluation of the photoswitching performance showed that **SubPc-DE$_1$** is likely to decompose during photocyclization and cycloreversion. This tendency was also observed through significative modifications in their ^{1}H NMR spectra. From the NICS(0) values, the lower photoreactivity of **SubPc-DE$_1$** could be explained in term of significant contribution of aromatic feature of the pyrrole ring bonded to the two thiophene rings. TD-DFT reveals that HOMO and LUMO of **SubPc-DE$_1$** are antisymmetric, suggesting the photocyclization occurred by an unusual manner.

Acknowledgements

This work was partly supported by JSPS KAKENHI Grant Numbers JP23H04876 and JP22H05134 for Transformative Research Area (A), JP24K08361 for Scientific Research (C) (M.Y.), JP22H00325 for Scientific Research (A) (GR), and JP22H02052 for Scientific Research (B) (T.K.). This work was achieved thanks to the facilities of NAIST-Center of Materials Platform (CMP). The University Paul Sabatier (Toulouse) and NAIST are also warmly thanked for

providing a crossed position to GR. We are also grateful to Dr. Claire Kammerer for fruitful discussions.

Keywords: Subphthalocyanine • Porphyrinoids • Diarylethene • Photochromism • DFT calculation

[1] a) M. Irie, M. Mohri, *J. Org. Chem*. **1998**, *53*, 803; b) M. Irie, *Chem. Rev*. **2000**, *100*, 1685; c) M. Irie, T. Fukaminato, K. Matsuda, S. Kobatake, *Chem. Rev*. **2014**, *114*, 12174; d) F. Yu, W. Liu, B. Li, D. Tian, J. Zuo, Q. Zhang, *Angew. Chem. Int. Ed*. **2019**, *58*, 16101.

[2] a) M. Irie, S. Kobatake, M. Horichi, *Science*. **2000**, *291*, 1769; b) K. Shibata, K. Muto, S. Kobatake, M. Irie, *J. Phys. Chem. A*. **2002**, *106*, 209; c) S. Kobatake, K. Uchida, E. Tsuchida, M. Irie, *Chem. Commun*. **2002**, 2804.

[3] a) T. Kawai, T. Sasaki, M. Irie, *Chem. Commun*. **2001**, 711; b) M. Irie, T. Fukaminato, T. Sasaki, N. Tamai, T. Kawai, *Science*. **2002**, *420*, 759; c) T. Fukaminato, T. Doi, N. Tamaoki, K. Okuno, Y. Ishibashi, H. Miyasaka, M. Irie, *J. Am. Chem. Soc*. **2011**, *133*, 4984.

[4] a) J. Zhang, H. Tian, *Adv. Optical. Mater*. **2018**, 6, 1701278; b) A. M. Krayushkin, S. N. Ivanov, A. Y. Martynkin, B. V. Lichitsky, A. A. Dudinov, B. M. Uzhinov, *Russ. Chem. Bull*. **2001**, *50*, 116e21; c) M. M. Krayushkin, S. N. Martynkin, B. V. Lichitsky, A. A. Dudinov, B. M. Uzhinov, *Russ. Chem. Bull*. **2001**, *50*, 116; d) T. Kawai, T. Iseda, M. Irie, *Chem. Commun*. **2004**, 72; e) S. Fukumoto, T. Nakashima, T. Kawai, *Angew. Chem. Int. Ed*. **2011**, *50*, 1; f) S. Fukumoto, T. Nakashima, T. Kawai, *Eur. J. Org. Chem*. **2011**, 5047; g) S. Fukumoto, T. Nakagawa, S. Kawai, T. Nakashima, T. Kawai, *Dyes and Pigments* **2011,** *89*, 297; h) S. Fukumoto, T. Nakashima, T. Kawai, *Dyes and Pigments* **2012**, *92*, 868; i) H-L. Wong, C-C, Ko, W. H. Lam, N. Zhu, V. W. W. Yam, *Chem. Eur. J*. **2009**, *15*, 10005; j) G. Gavrel, P. Yu, A. Léaustic, R. Guillot, R. Métivier and K. Nakatani, *Chem. Commun.* **2012**, *48*, 10111; k) R. Li, Q. Fang, M. Chen, M. Yamada, Y. Tsuji, Y. Kugai, W. Li, T. Kawai, *Chem. Eur. J*. **2023**, *29*, e202302693; l) G. Gavrel, P. Yu, A. Léaustic, R. Guillot, R. Métivier and K. Nakatani, *Chem. Commun*. **2012**, *48*, 10111.

[5] a) H. Tian, B. Chen, H. Tu, K. Müllen, *Adv. Mater*. **2002**, *14*, 918; b) Q. Luo, B. Chen, M. Wang, H. Tian, *Adv. Funct. Mater*. **2003**, *13*, 233.

[6] M. Yamada, T. Sawazaki, M. Fujita, F. Asanoma, Y. Nishikawa, T. Kawai, *Chem. Eur. J*. **2022**, *28*, e202201286.

[7] A. Meller, A. Ossko, *Monatsh. Chem.* **1972**, *103*, 150.

[8] G. Lavarda, J. Labella, M. V. Martinez-Diaz, M. S. Rodriguez Morgade, A. Osuka, T. Torres, *Chem. Soc. Rev*. **2022**, *51*, 9482.

[9] S. Shimizu, N. Kobayashi, *Chem. Commun*. **2014**, *50*, 6949.

[10] M. Shi, J. Chen, Z. Shen, *J. Porphyr. Phthalocyanines.* **2016**, *20*, 1.

[11] E. Cañizares-Espada, G. Pérez de Bustos, K. Naoda, A. Osuka, T. Torres, M. S. Rodríguez-Morgade, *Org. Lett*. **2024**, *26*, 955.

[12] H. Tian, H-Y. Tu, *Adv. Mater*. **2000**, *12*, 1597.

[13] H.-P. Jacquot de Rouville, R. Garbage, F. Ample, A. Nickel, J. Meyer, F. Moresco, C. Joachim, G. Rapenne, *Chem. Eur. J.* **2012**, *18*, 8925.

[14] M V. Fulford, D. jaidka, A. S. Paton, G E. Morse, E R. L. Brisson, A J. Lough, T P. Bender, *J. Chem. Eng. Data*. **2012**, *57*, 2756.

[15] C. G. Claessens, D. González-Rodríguez, M. S. Rodríguez-Morgade, A. Medina, T. Torres, *Chem. Rev*. **2014**, *114*, 2192.

[16] C.G. Claessens, D. González-Rodríguez, B. del Rey, T. Torres, G. Mark, H.-P. Schuchmann, C. von Sonntag, J. G. MacDonald, R.S. Nohr, *Eur. J. Org. Chem.* **2003**, 2547.

[17] C. Wang, X. Chen, D. Qi, S. Bi, J. Jiang, *Inorg. Chem. Commun*. **2017**, *85*, 9.

[18] M. S. Rodríguez-Morgade, S. Esperanza, T. Torres, J. Barberá, *Chem. Eur. J*. **2005**, *11*, 354.

[19] 510-590 nm light and > 700 nm light irradiation was conducted on hexane solution of **SubPc-DE$_1$** (0.3×10^{-5} M, 200 ml) in a quartz flask and the solvent was removed under vacuum. Subsequently, ^{1}H NMR was measured in $CDCl_3$.

[20] Z. Chen, C S. Wannere, C. Corminboeuf, R. Puchta, P. v. R. Schleyer, *Chem. Rev*. **2005**, *105*, 3842.

[21] S. Kobatake, K. Uchida, E. Tsuchida, M. Irie, *Chem. Commun*. **2002**, 2804.

[22] Z. Luyang, Q. Dongdong, C. Xue, J. Jianzhuang, *Chin. J. Chem.* **2012**, *30*, 2126.

[23] a) I. Ikariko, S. Kim, Y. Hiroyasu, K. Higashiguchi, K. Matsuda, T. Hirose, H. Sotome, H. Miyasaka, S. Yokojima, M. Irie, S. Kurihara, T. Fukaminato, *J. Phys. Chem. Lett*. **2022**, *14*, 7429; b) I. Ikariko, S. Kim, Y. Hiroyasu, K. Higashiguchi, K. Matsuda, S. Yokojima, S. Kurihara, T. Fukaminato, *Chem. Lett*. **2022**, *51*, 1095.

[24] J. Massaad, J-C. Micheau, C. Coudret, C. L. Serpentini, G. Guirado, *Chem. Eur. J*. **2013**, *19*, 12435.

Supporting Information

I. Synthetic procedures

a. General information

Chemicals were purchased from Wako Pure Chemical Industries Ltd., Tokyo Chemical Industry Co., Ltd. (TCI), or Kanto Chemical Co., Inc. and used as received without further purification. NMR spectra were recorded on JEOL JNM-ECA600 (600 MHz) and JEOL JNM-ECZ500R (500 MHz). Silica gel column chromatography was performed using Silica gel 60N (spherical neutral, particle size 63-210 μm) or SILICYCLE Ultra-Pure Silica Gel (pH6.5-7.5, particle size 40-63 μm, 230-400 mesh). Recycling preparative HPLC separation was performed with a LaboACE LC-5060 (Japan Analytical Industry Co., Ltd.). Mass spectra were measured with mass spectrometers (JEOL JMS S3000 for MALDI). UV-vis absorption spectra were measured using a V-550, V-760 spectrometer. Light irradiation was carried out with a Shimadzu QYM-01. Fluorescence spectra were measured with a Jasco FP-8500. Calculations were performed with the Gaussian16 package. NICS(0) values were calculated by the gauge-independent atomic orbital (GIAO method) at the B3LYP/6-31+G(d,p) level of theory. Emission quantum yield was measured by using a Hamamatsu Photonics C9920-02 instrument with an integrating sphere.

b. Synthesis

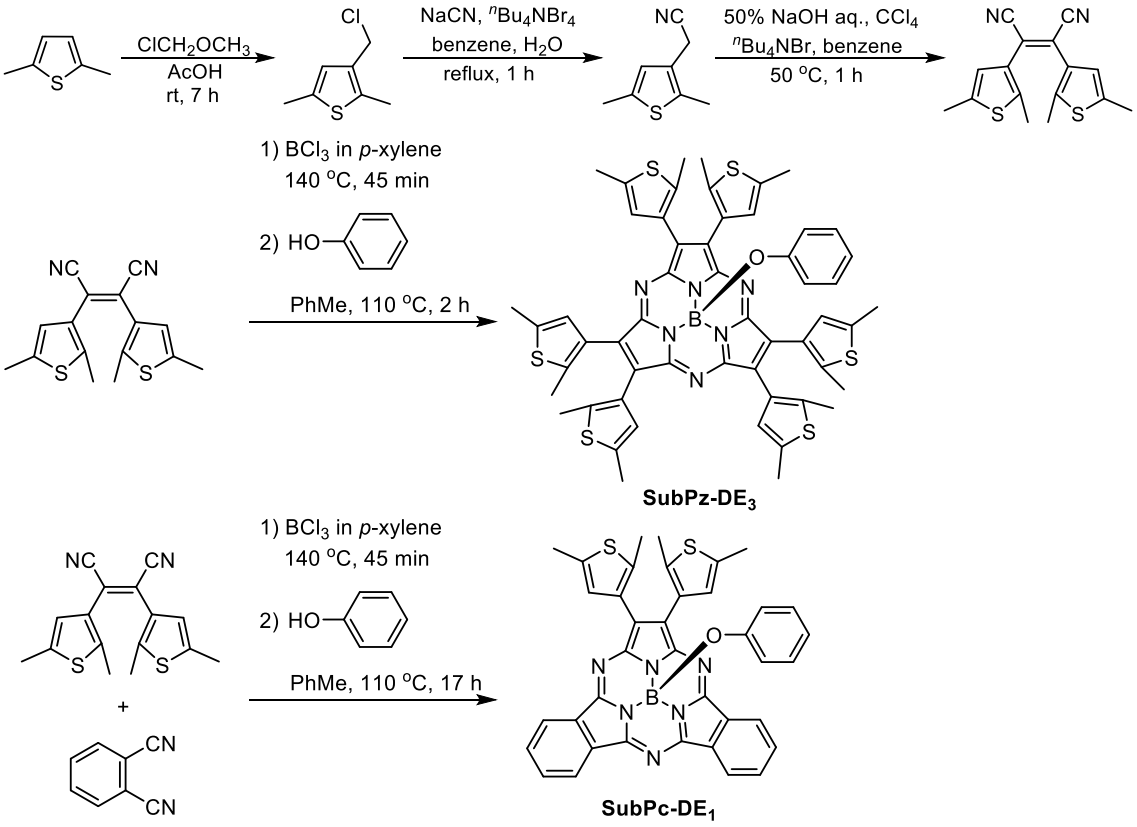

3-(Chloromethyl)-2,5-dimethylthiophene

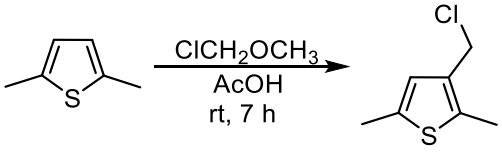

2,5-dimethylthiophene (48 g, 0.43 mol, 1.0 eq.) was added to AcOH (113 ml) under argon. Chloromethyl methyl ether (34 g, 0.42 mol, 1.0 eq.) was added dropwise to the solution. The mixture was stirred for 7 h at room temperature. The color of the mixture changed from green to blue. The resulting solution was poured into water (200 ml), stirred for ten minutes and extracted with $CHCl_3$ (200 ml × 3). The combined organic layer was washed with saturated $NaHCO_3$ aqueous solution (200 ml × 2), dried over anhydrous $MgSO_4$, filtered, and evaporated in vacuo. The obtained crude (67 g) was used for the next reaction without further purification.

2,5-Dimethyl-3-thiopheneacetonitrile[S1]

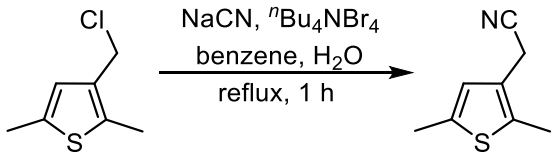

A mixture of crude 3-(chloromethyl)-2,5-dimethylthiophene (67 g), benzene (62 ml), sodium cyanide (32 g), and tetrabutylammonium bromide (4.0 g) in water (120 ml) was refluxed for 1 h. After cooling at room temperature, the reaction mixture was extracted with $CHCl_3$ (200 ml × 4), dried over anhydrous $MgSO_4$, filtered, and evaporated. The residue was purified by distillation under reduced pressure (12-15 HPa, bp:120-130 °C) to give the 2,5-dimethyl-3-thiopheneacetonitrile (25 g) as a pale-yellow oil which was used for the next reaction without further purification.

(2*Z*)-2,3-Bis(2,5-dimethyl-3-thienyl)-2-butenedinitrile[S2] [S3]

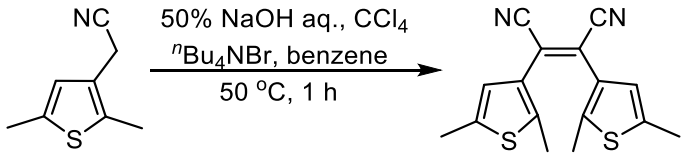

To 310 ml of 50% NaOH aqueous solution containing tetrabutylammonium bromide (930 mg) was added a mixture of 2,5-dimethyl-3-thiopheneacetonitrile (25 g), benzene (310 g) and CCl_4 (310 g). The solution was stirred for 1 h at 50 °C. The reaction mixture was poured into water (1 L), extracted with $CHCl_3$ (200 ml × 3), dried over anhydrous $MgSO_4$, filtered, and evaporated. The crude product was purified by silica gel chromatography (toluene/hexane = 50:1 followed by pure toluene). The final compound was further purified by rinsing with hexane to give (2*Z*)-2,3-bis(2,5-dimethyl-3-thienyl)-2-butenedinitrile (5.44 g, 18.2 mmol) with an overall 8% for the three steps.

^{1}H NMR (500 MHz, $CDCl_3$, 298 K) δ: 6.35 (s, 2H), 2.33 (s, 6 H), 2.14 (s, 6 H)

SubPz-DE$_3$

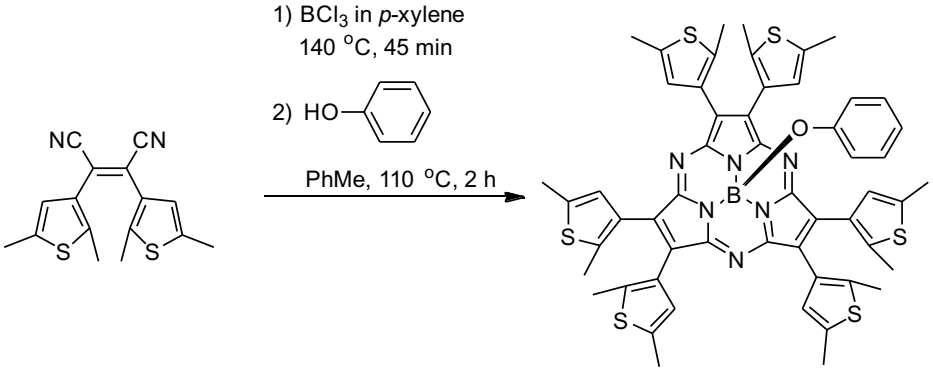

SubPz-DE$_3$

A solution of BCl_3 in *p*-xylene (1 M, 2.5 ml, 2.5 mmol, 1.0 eq.) was added under argon to (2*Z*)-2,3-bis(2,5-dimethyl-3-thienyl)-2-butenedinitrile (717 mg, 2.45 mmol, 1.0 eq.), and the mixture was stirred at 140 °C for 45 min. After removing the solvents, phenol (1.14 g, 12.1 mmol, 4.9 mmol) in toluene (3.4 ml) was added to the residue. The resulting solution was stirred at reflux for 2 h. After evaporation of the solvent, the crude was purified by silica gel chromatography (toluene). The final compound was further purified by GPC with $CHCl_3$ as eluent to afford **SubPz-DE$_3$** as a pink solid (1.86 mg, 1.86 μmol, 0.2%).

^{1}H-NMR (500MHz, $CDCl_3$) δ: 6.83 (m, 2H, *m*-phonoxy), 6.76 (s, 6H), 6.66 (t, 1H, J = 7.5 Hz, *p*-phenoxy), 5.44 (d, 2H, J = 7.7 Hz, *o*-phenoxy), 2.44 (s, 18H), 2.37 (s, 18H)
HR-MALDI-TOF-MS: *m/z* calculated for $[BC_{54}H_{47}N_6OS_6]^+$ 998.2232; found 998.2228 $[M]^+$

SubPc-DE$_1$

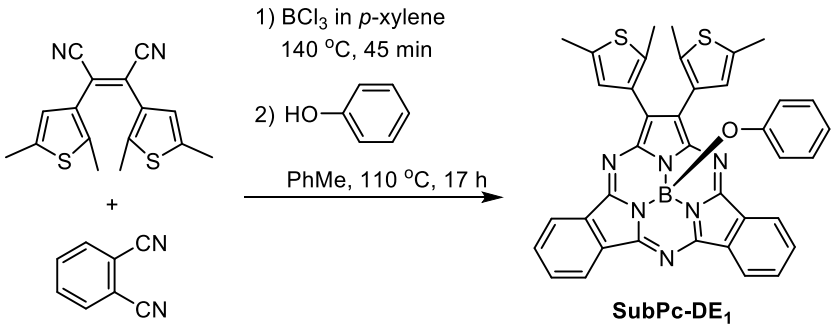

SubPc-DE$_1$

A solution of BCl_3 in *p*-xylene (1 M, 3.0 ml, 3.0 mmol, 3.0 eq.) was added under argon to (2*Z*)-2,3-bis(2,5-dimethyl-3-thienyl)-2-butenedinitrile (300 mg, 1.0 mmol, 1.0 eq.) and 1,2-dicyaniebenzene (240 mg, 2.03 mmol, 2.0 eq.). The reaction mixture was stirred at 140 °C for 45 min. After removing the solvent, phenol (1.04 g, 11 mmol) in toluene (10 ml) was added to the residue. The resulting solution was stirred at reflux for 17 h. After evaporation of the solvent, the crude product was purified by silica gel chromatography (CH_2Cl_2/hexane = 20:1). The final compound was further purified by GPC with $CHCl_3$ as eluent to afford **SubPc-DE$_1$** as a thick purple solid (4.7 mg, 7.2 μmol, 0.7%).
^{1}H NMR ($CDCl_3$, 600 MHz) δ: 8.80 (m, 4H), 7.91 (m, 4H), 6.79 (m, 2H, *m*-phenoxy), 6.69 (s, 2H), 6.64 (t, 1H, J = 7.6 Hz, *p*-phenoxy), 5.45 (d, 2H, J = 8.2 Hz, *o*-phenoxy), 2.47 (s, 6H), 2.38 (s, 6H)
^{13}C NMR ($CDCl_3$, 151 MHz) δ: 155.7, 152.8, 151.8, 151.5, 137.1, 135.8, 132.4, 131.1, 130.6, 130.1, 129.0, 128.9, 127.9, 127.9, 122.6, 122.6, 121.3, 119.0, 15.4, 14.6

HR-MALDI-TOF-MS: m/z calculated for $[BC_{38}H_{27}N_6OS_2]^+$ 658.1776; found 658.1782 $[M]^+$
UV-vis ($CHCl_3$): λ_{max} (ε) :575 nm (4.0×10^4 M^{-1} cm^{-1})

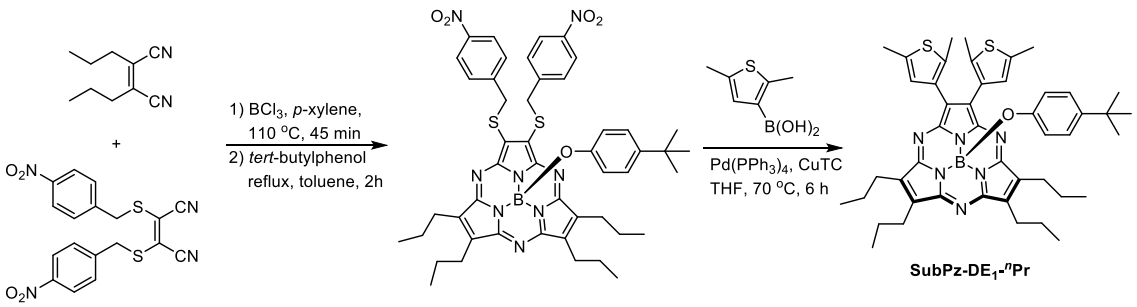

Scheme S1. The synthesis of **SubPz-DE$_1$-^{n}Pr**.[S4]

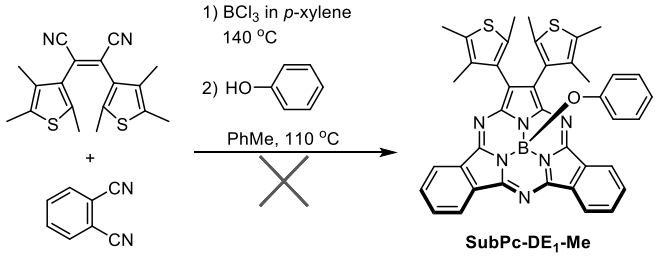

Scheme S2. Tentative (failed) synthesis of the permethylated thiophene derivative **SubPc-DE$_1$**

II. **Characterizations**

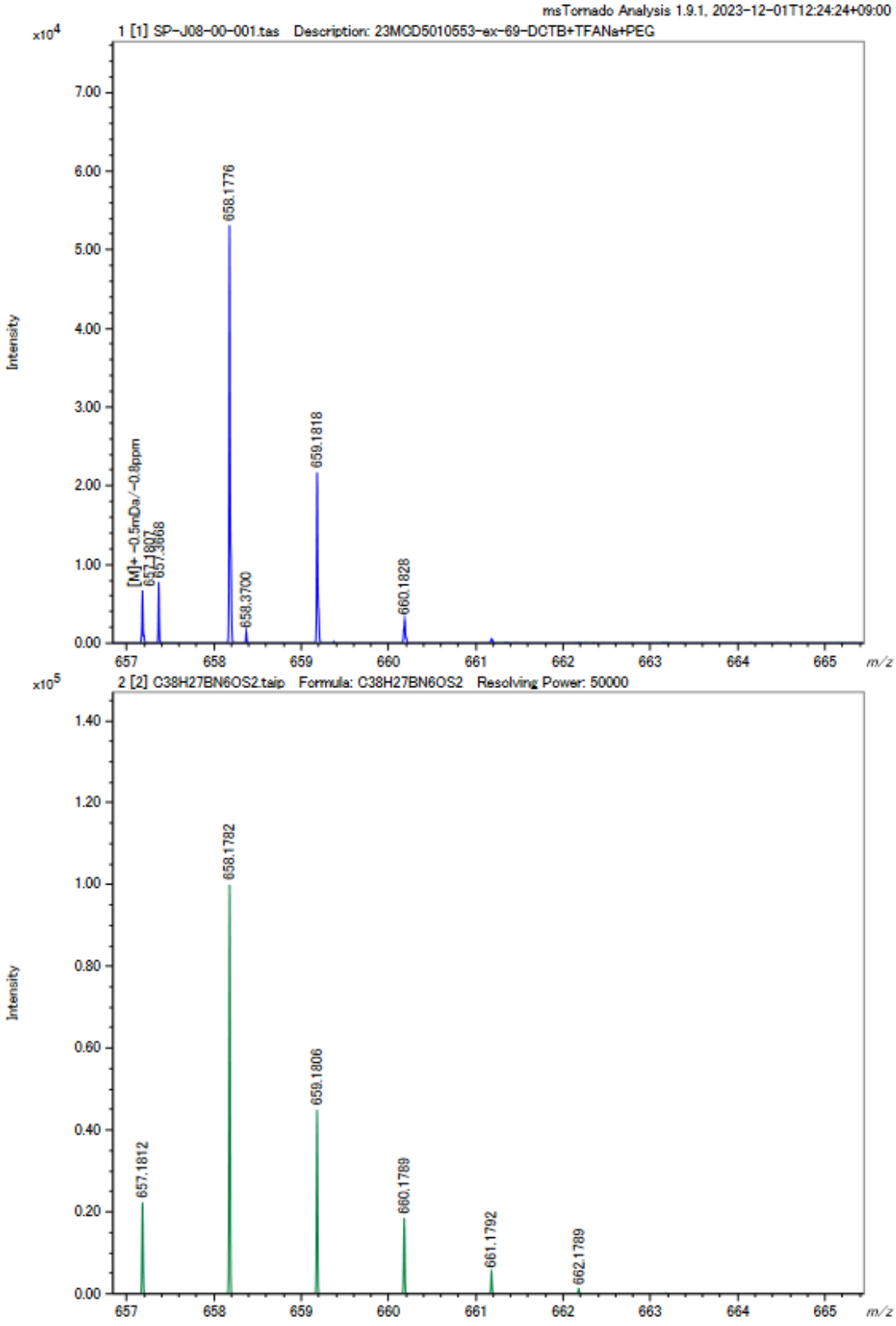

Figure S1. HR-MS (MALDI-TOF-MS, matrix: DCTB): measured (top) and calculated (bottom) isotopic pattern of **SubPc-DE$_1$**.

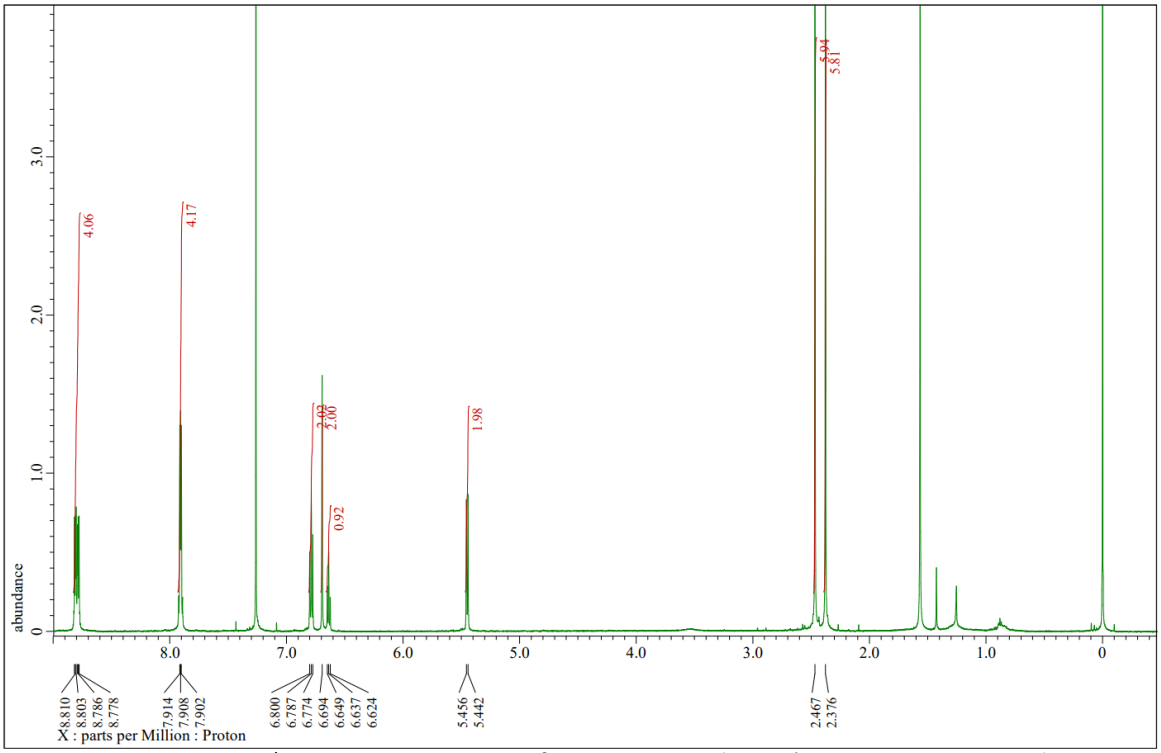

Figure S2. ^{1}H NMR spectrum of **SubPc-DE$_1$** ($CDCl_3$, 298 K, 500 MHz).

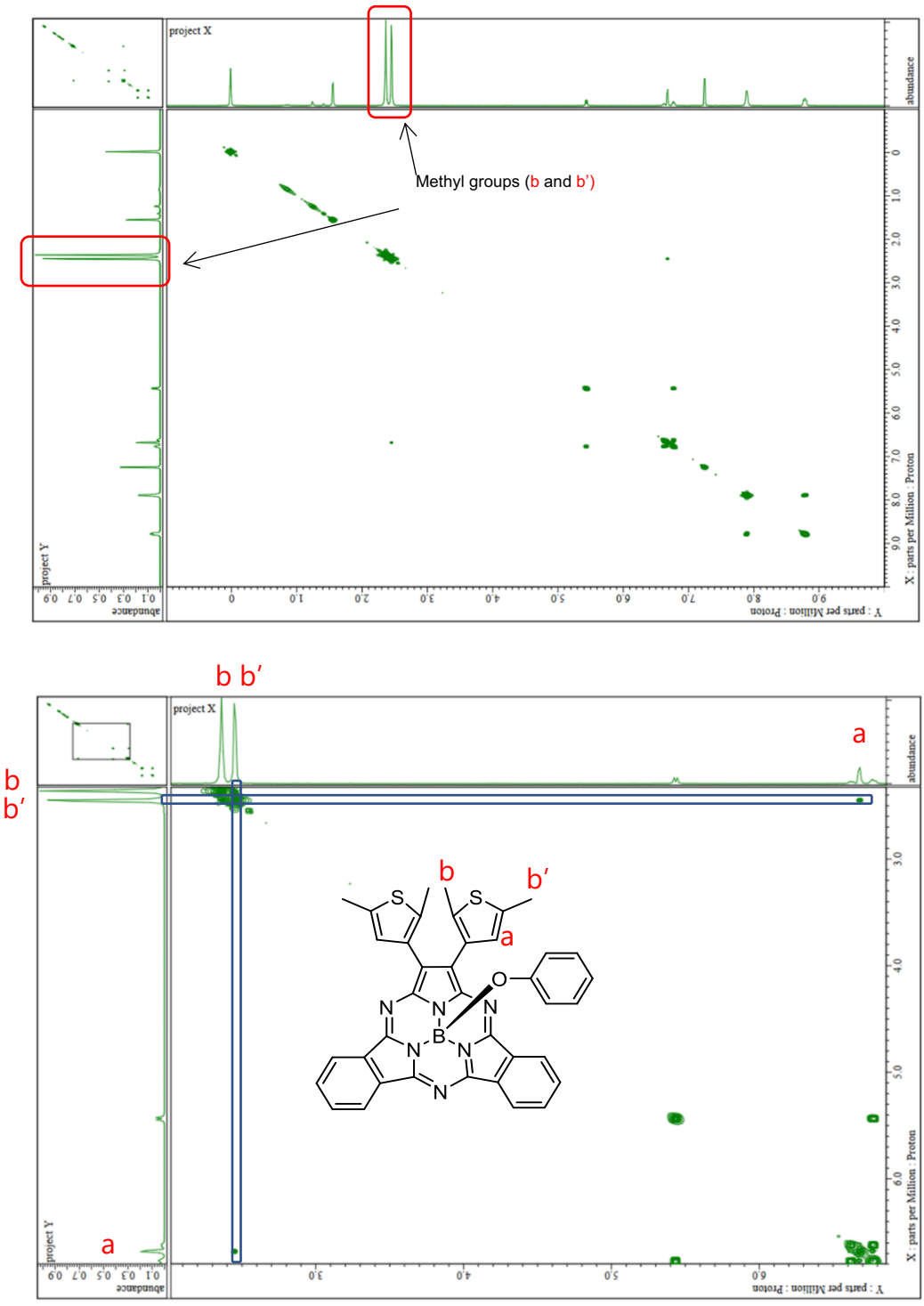

Figure S3. ^{1}H-^{1}H COSY spectrum of **SubPc-DE$_1$** ($CDCl_3$, 298K, 600 MHz). Full spectrum (top) and zoom for the 2-7 ppm region (bottom).

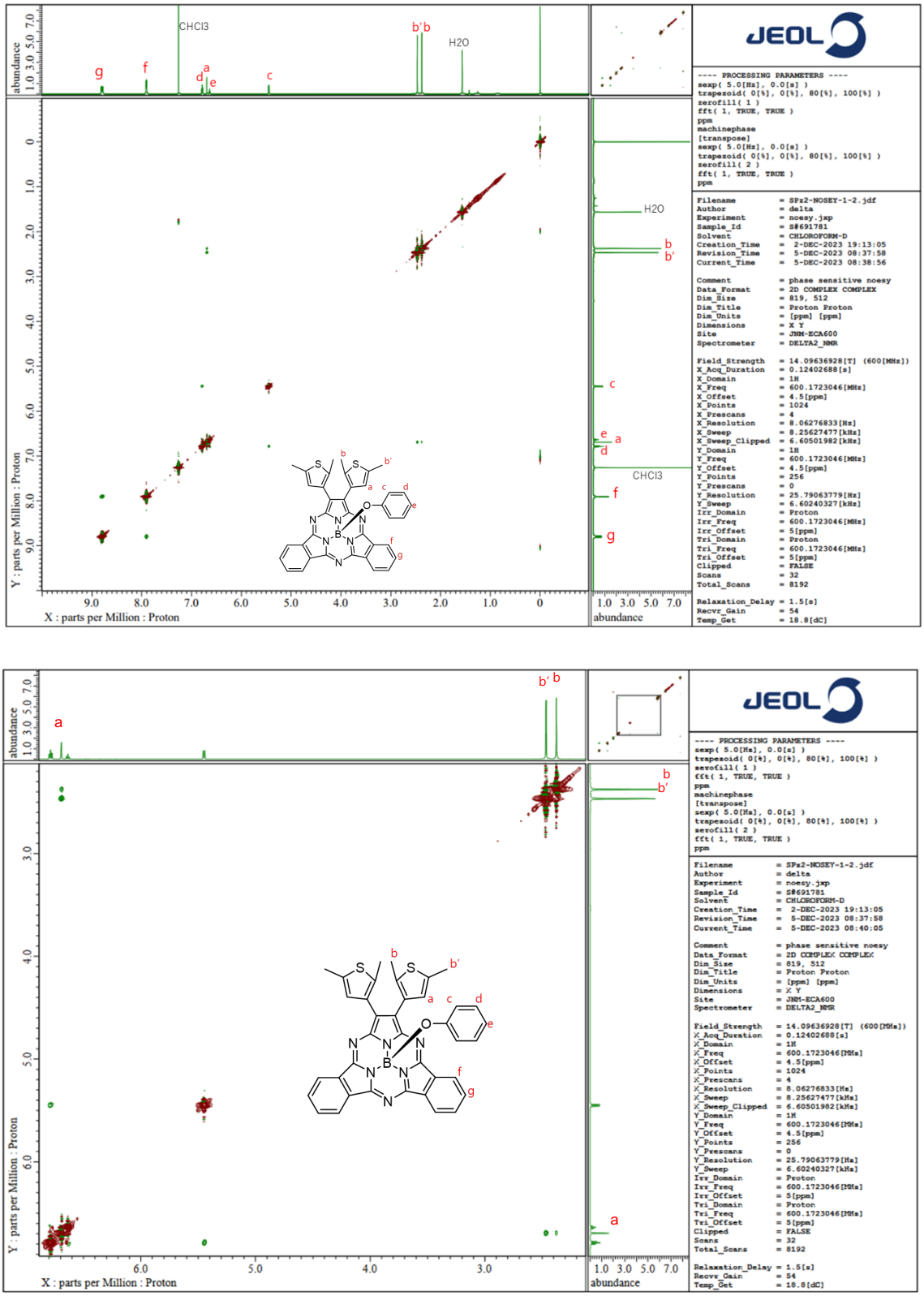

Figure S4. ^{1}H-^{1}H NOESY spectrum of **SubPc-DE$_1$** ($CDCl_3$, 298K, 600 MHz). Full spectrum (top) and zoom for the 2-7 ppm region (bottom).

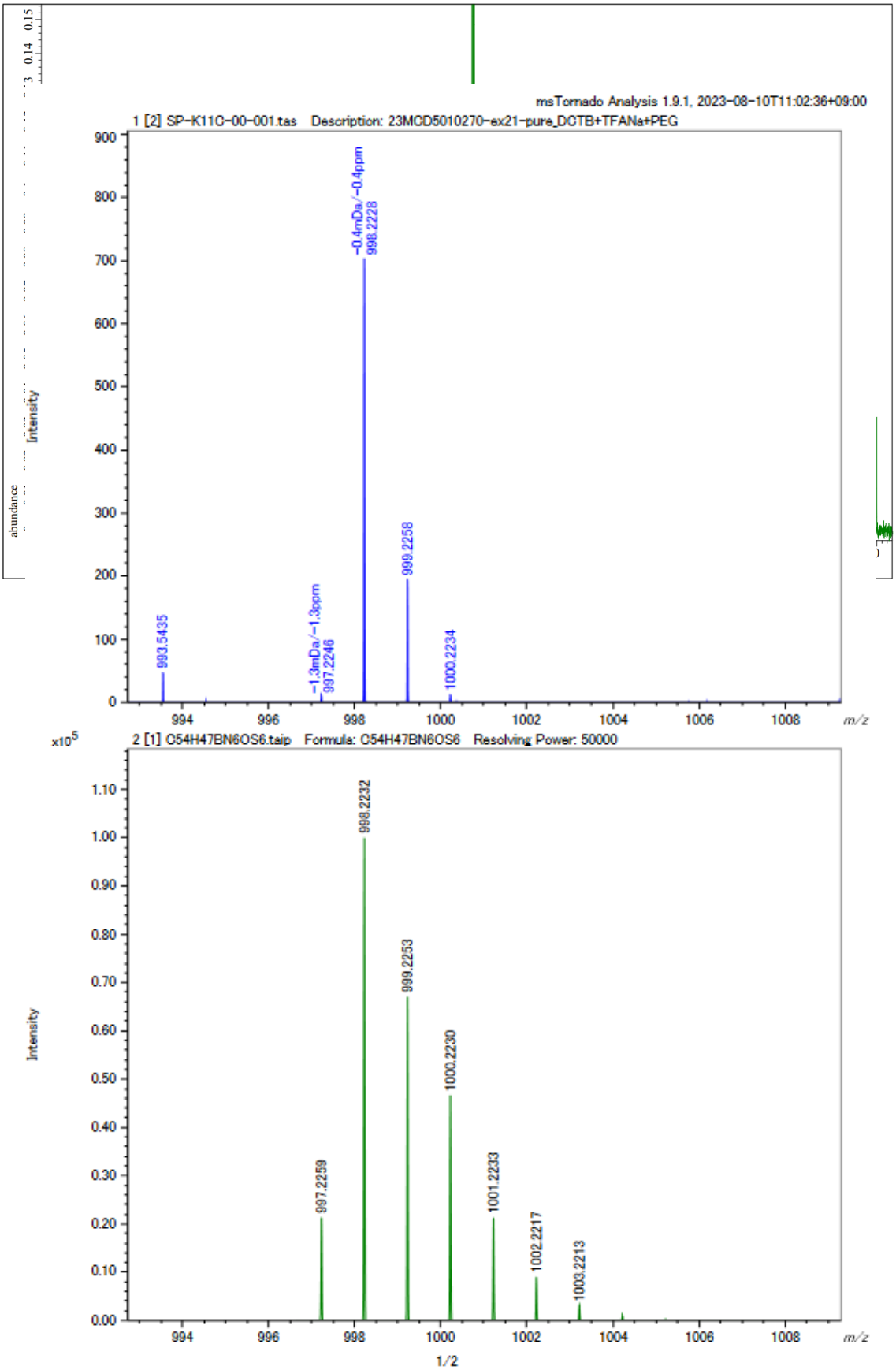

Figure S6. HRMS (MALDI-TOF-MS, matrix: DCTB): measured (top) and calculated (bottom) isotopic pattern of **SubPz-DE$_3$**

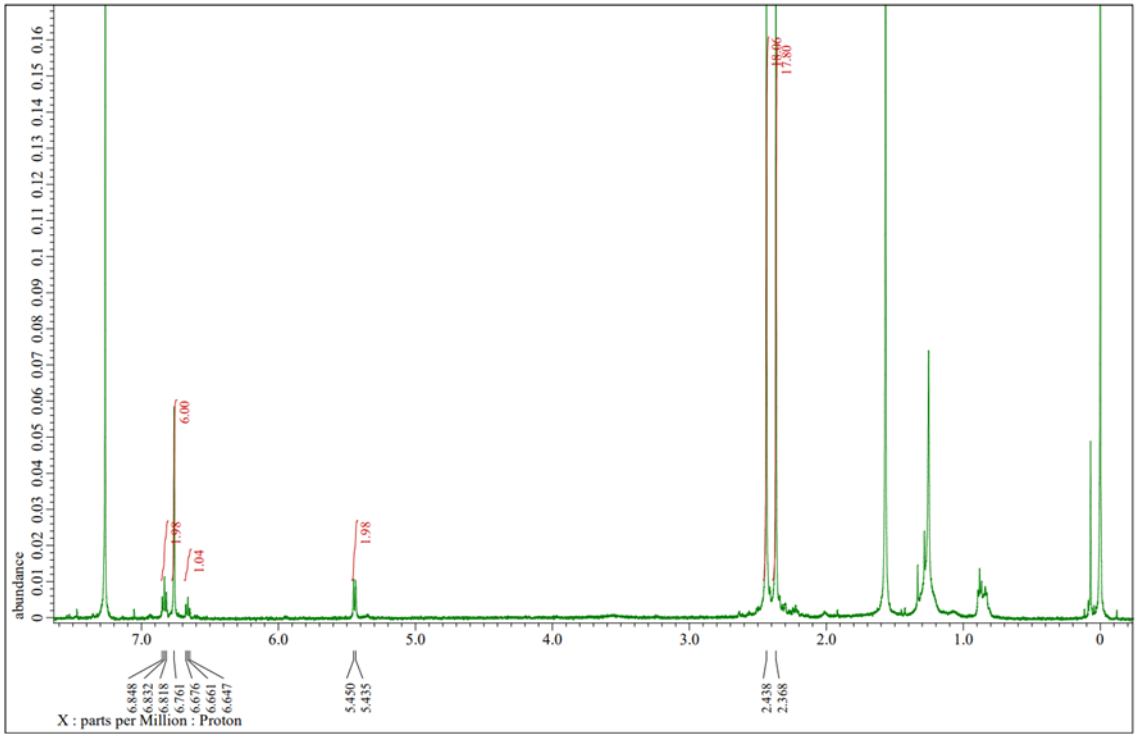

Figure S7. ^{1}H-NMR spectrum of **SubPz-DE$_3$** ($CDCl_3$, 298 K, 500 MHz)

III. Optical properties

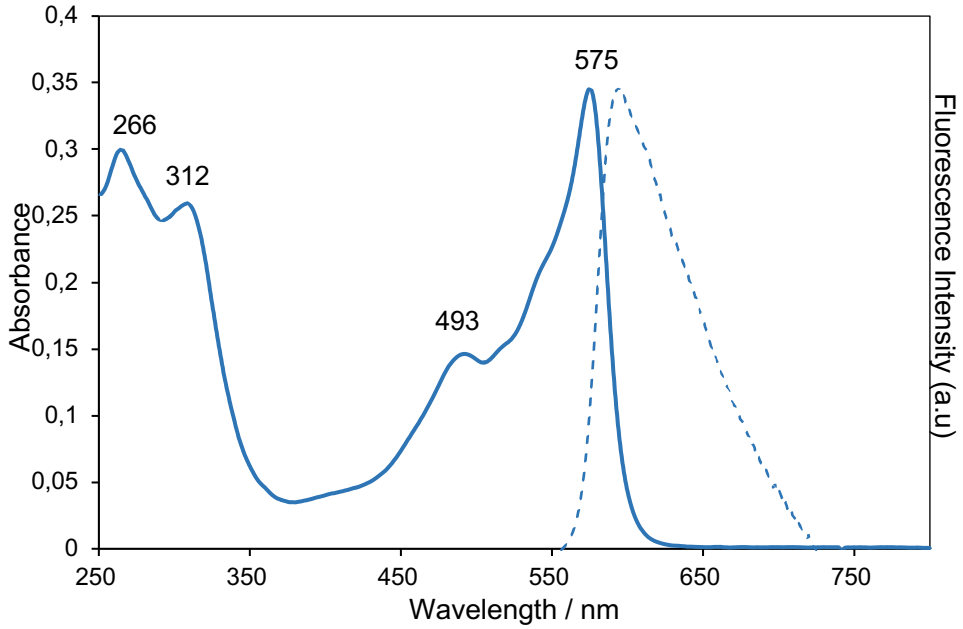

Figure S8. The UV-vis absorption and fluorescence spectra of **SubPc-DE$_1$** in chloroform (1.0×10^{-5} M, excitation wavelength: 400 nm)

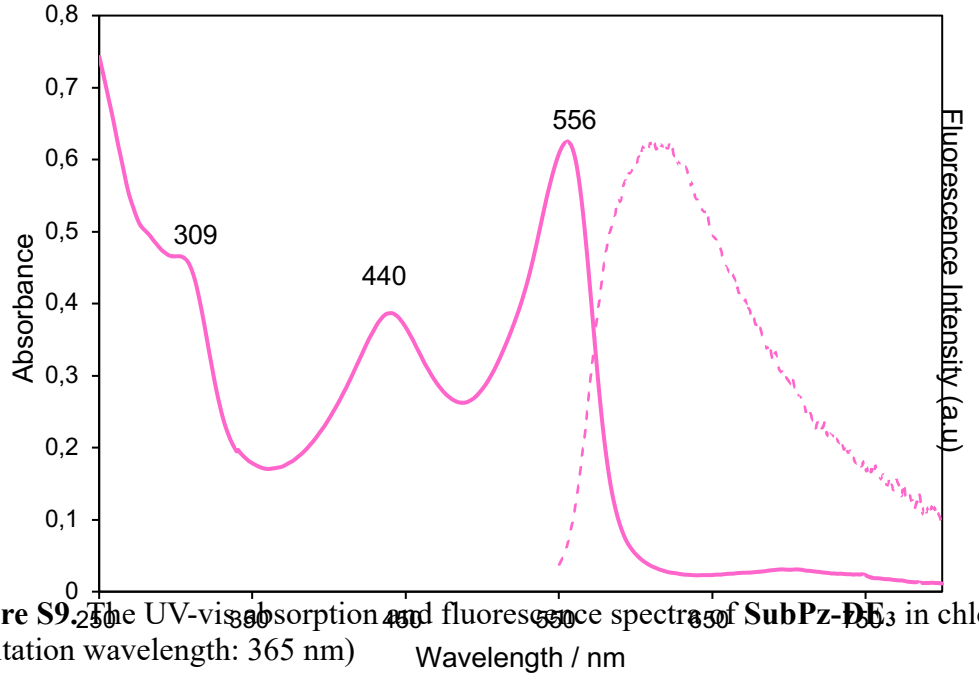

Figure S9. The UV-vis absorption and fluorescence spectra of **SubPz-DE$_3$** in chloroform (excitation wavelength: 365 nm)

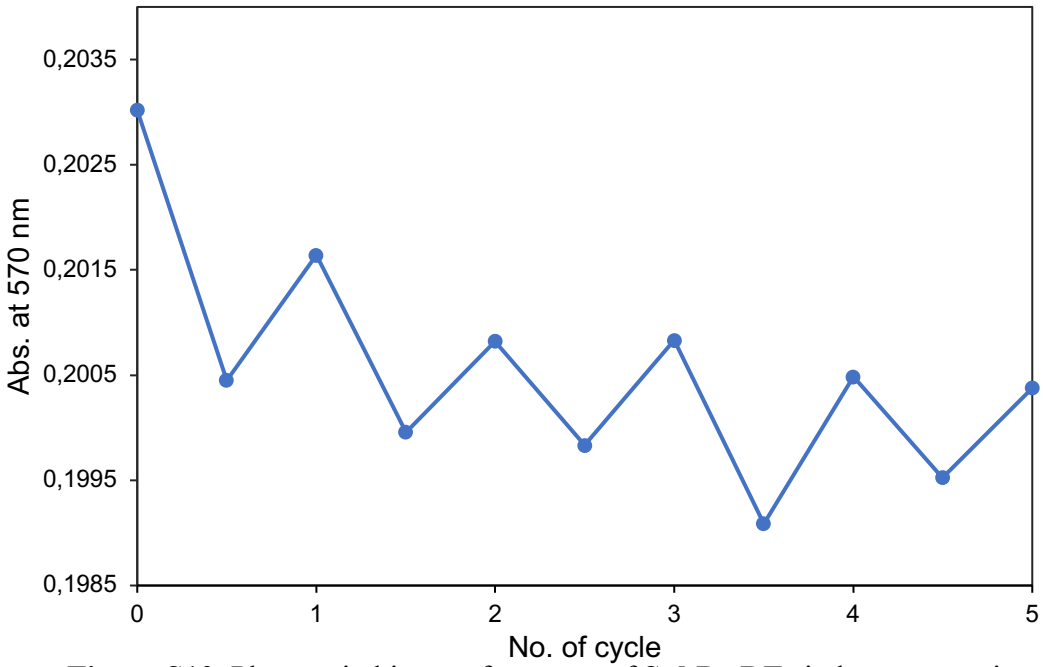

Figure S10. Photoswitching performance of **SubPc-DE$_1$** in hexane monitored by UV-vis absorbance at Q-band (570 nm).

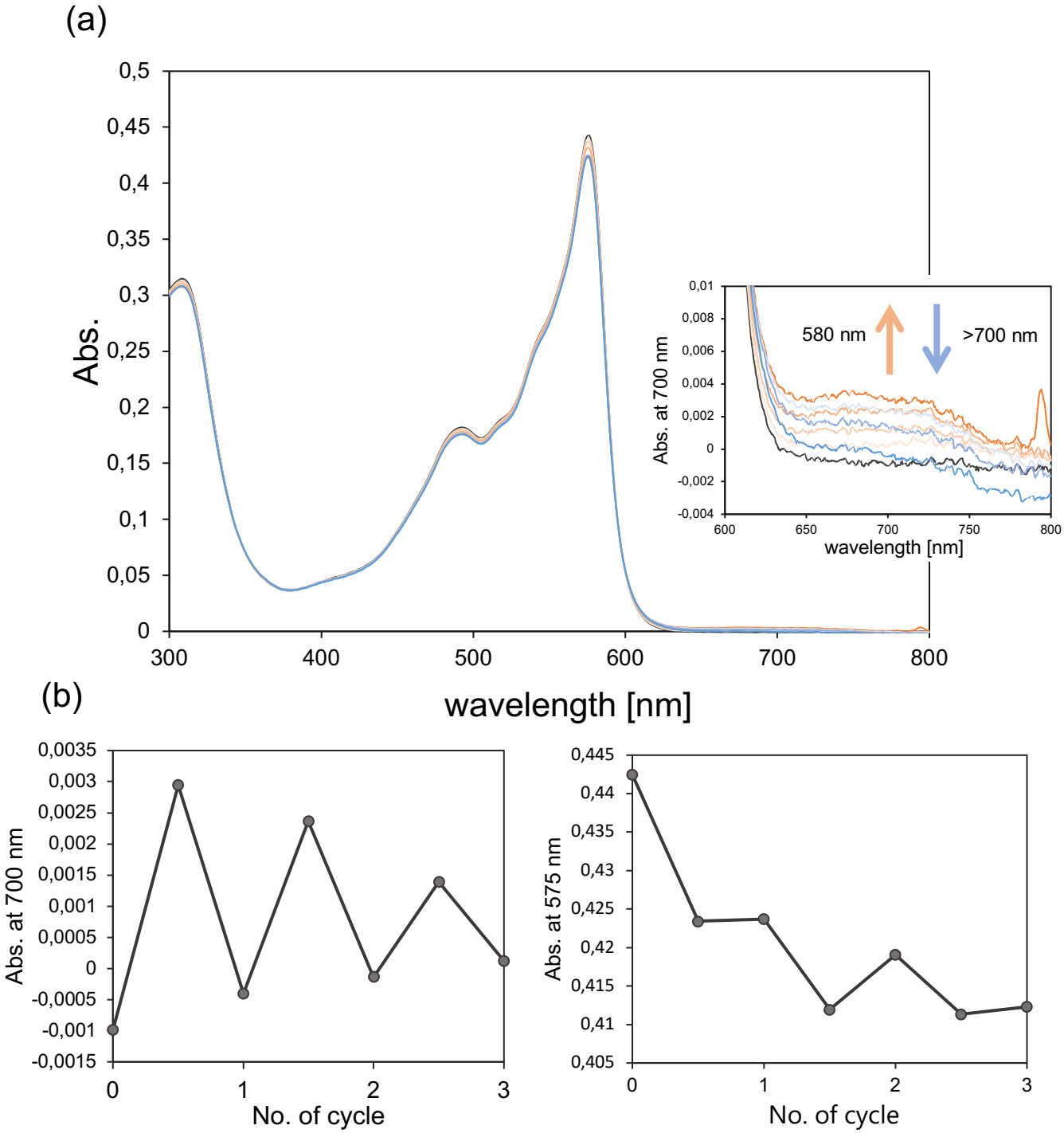

Figure S11. (a) The UV-vis absorption spectral change of in **SubPc-DE$_1$** in chloroform (1.1×10^{-5} M). Irradiation with 580 nm until the photostationaly state, and following >700 nm light irradiation. (b) Photoswitching performance of **SubPc-DE$_1$** in chloroform monitored by UV-vis absorbance at 575 nm and 700 nm.

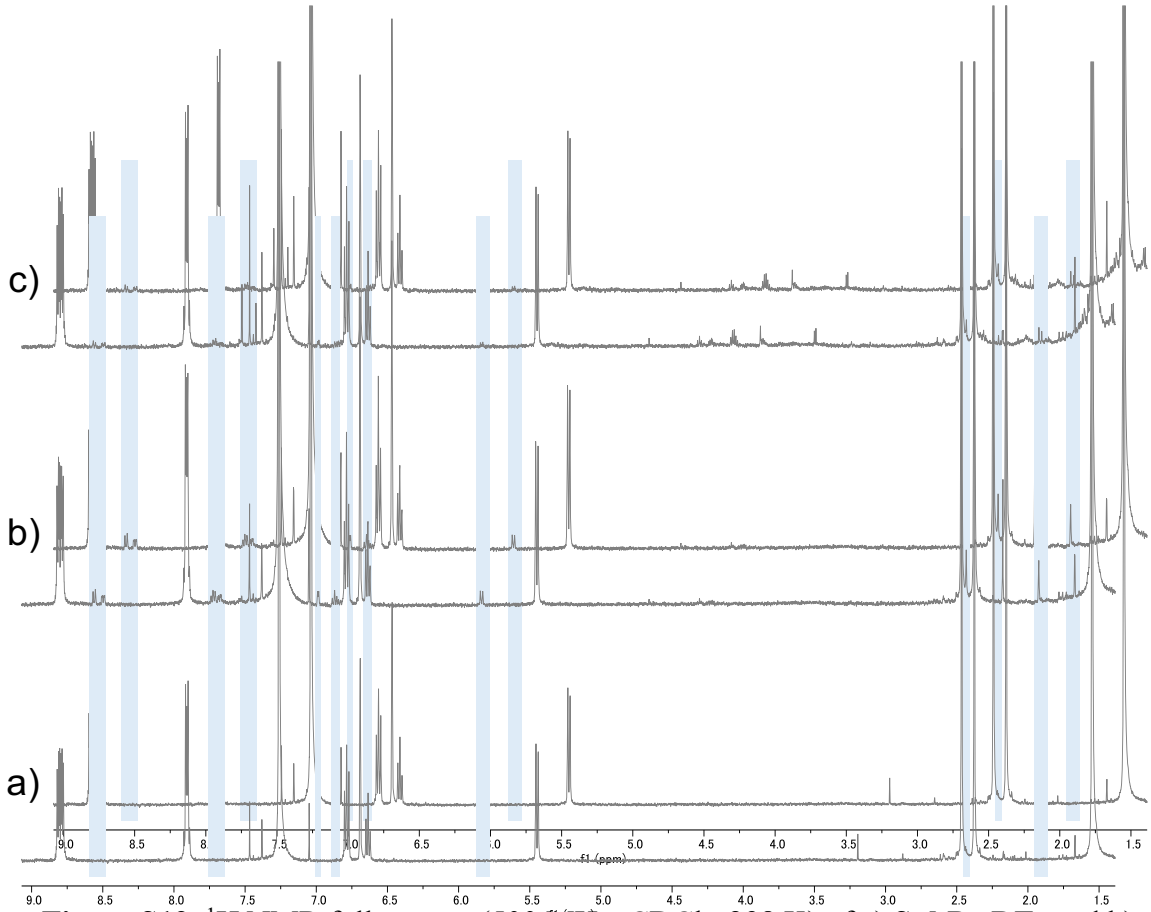

Figure S12. ^{1}H NMR full spectra (500 MHz, $CDCl_3$, 298 K) of a) **SubPc-DE$_1$** and b) after 510-590 nm light irradiation and c) after following > 700 nm light irradiation.

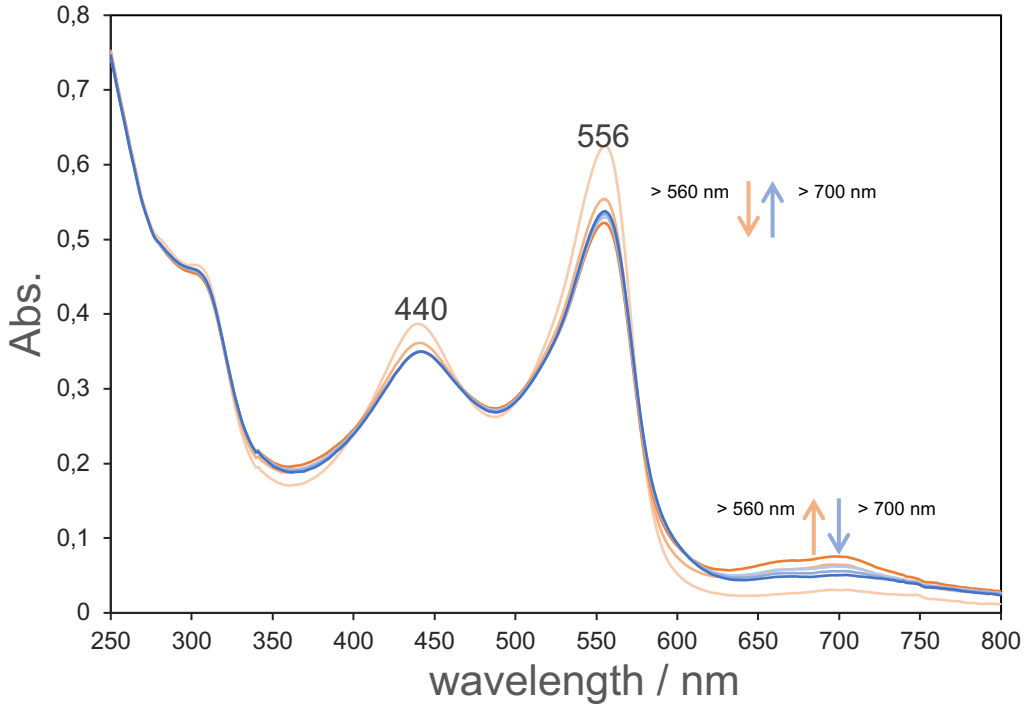

Figure S13. The UV-vis absorption spectral change of in **SubPz-DE$_3$** in chloroform. Irradiation with > 560 nm and following > 700 nm light irradiation.

IV. DFT calculation

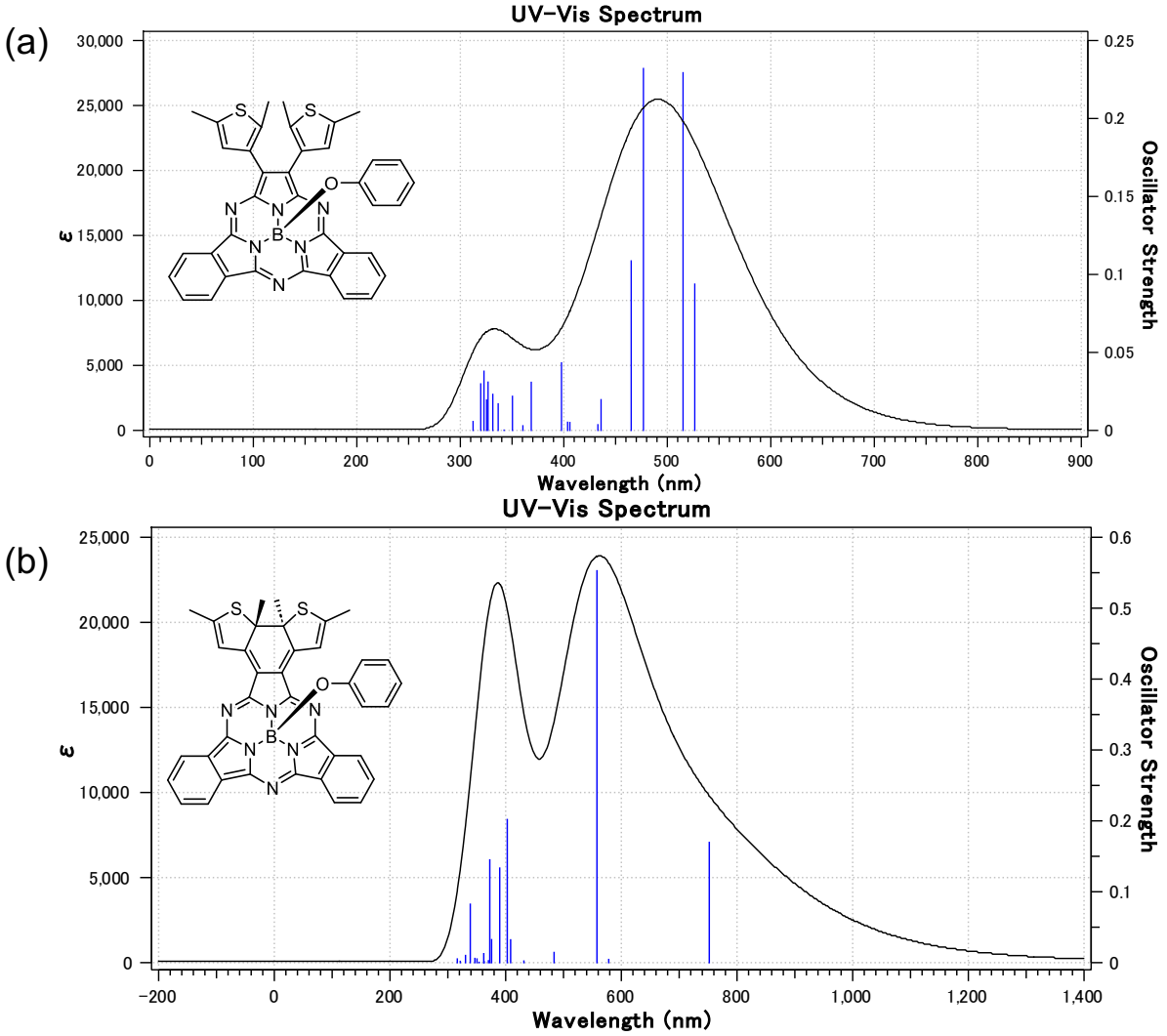

Figure S14. TD-DFT predicted absorption spectra for (a): the open form and (b): closed form of **SubPc-DE$_1$**. DFT calculation level: B3LYP/6-31+G(d,p)

Transition	f	Main contributions
$S_0 \rightarrow S_1$ (526.48 nm)	0.098	HOMO - 1 → LUMO (65%) HOMO → LUMO (30%) HOMO → LUMO + 1 (2%)

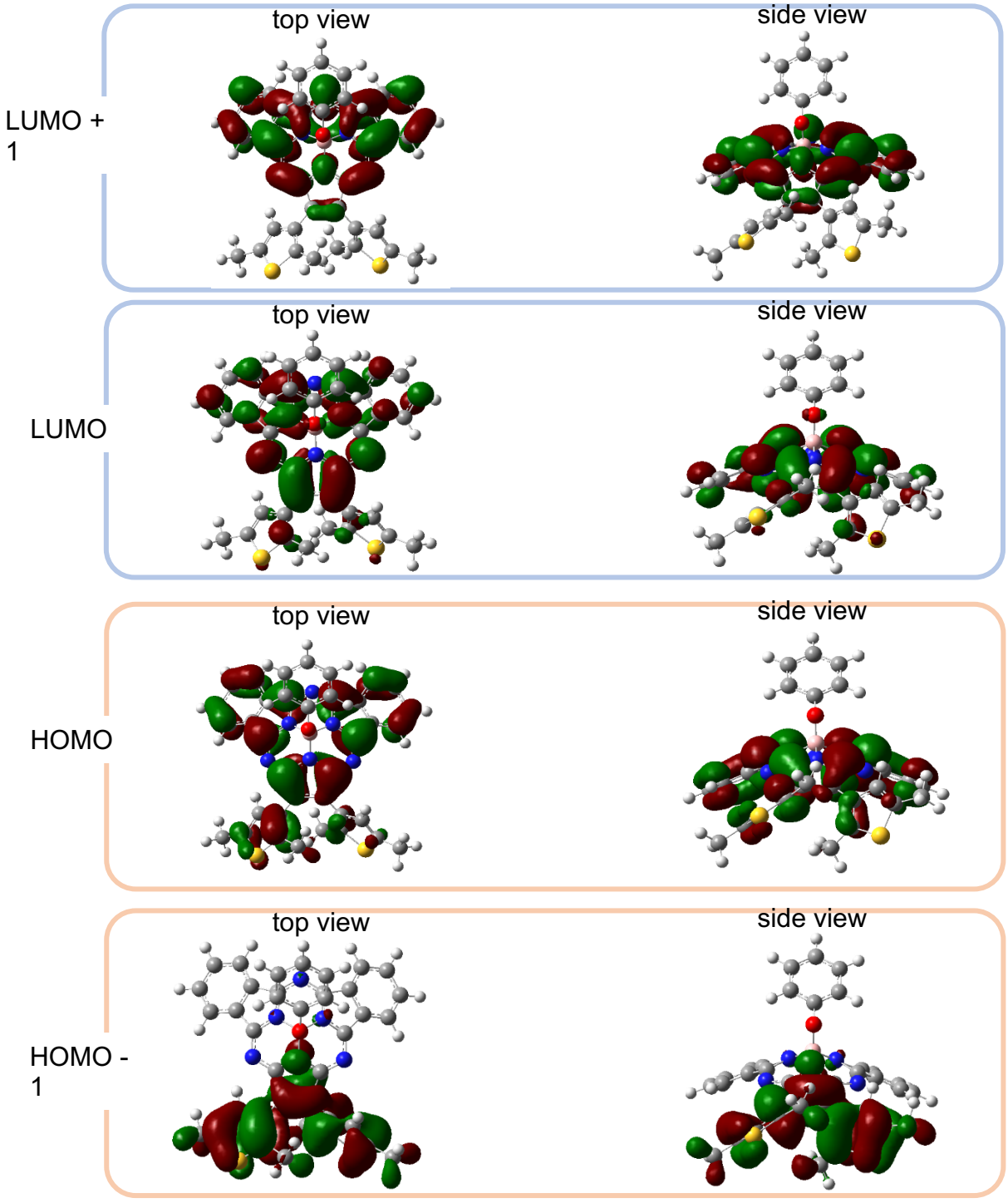

Figure S15. Oscillator strengths (f), dominant molecular orbital composition of $S_0 \rightarrow S_1$ transition and HOMO + 1, HOMO, LUMO, LUMO - 1 for **SubPc-DE$_1$**. DFT calculation level: B3LYP/6-31+G(d,p)

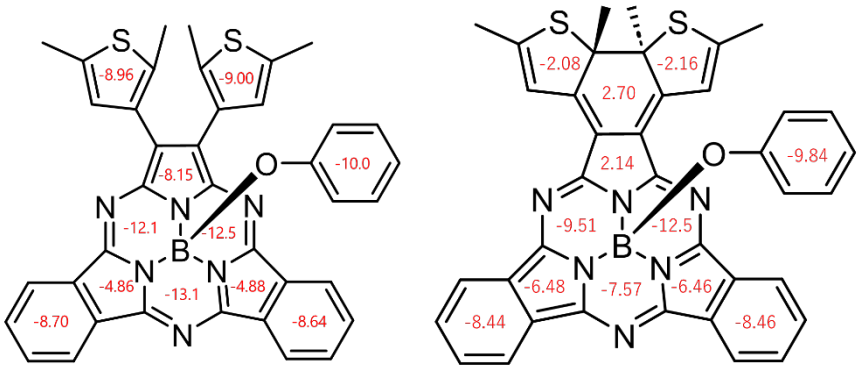

Figure S16. NICS(0) of **SubPc-DE$_1$** (open, closed form). DFT calculation level: B3LYP/6-31+G(d,p)

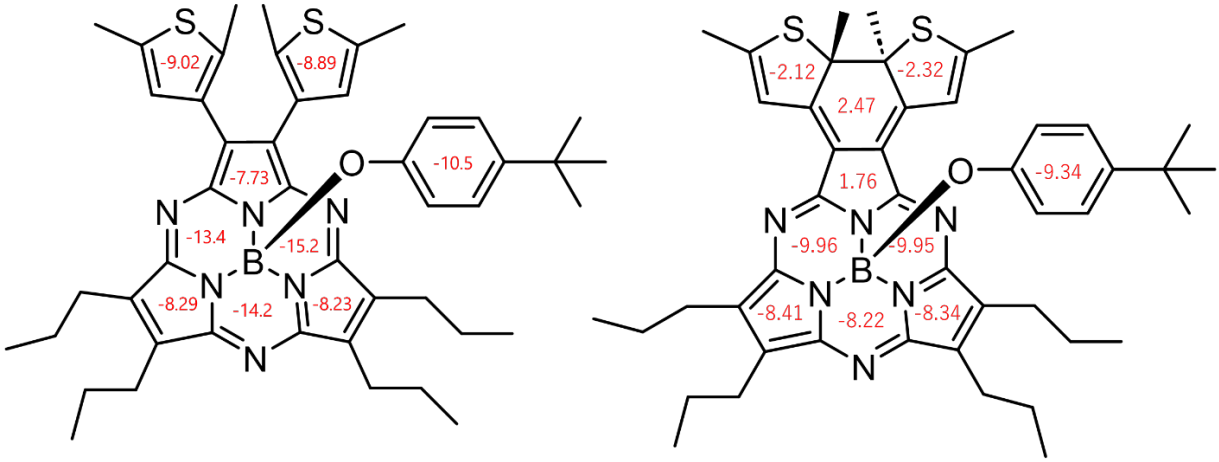

Figure S17. NICS(0) of **SubPz-DE$_1$-^{n}Pr** (open, closed form). DFT calculation level: B3LYP/6-31+G(d,p)

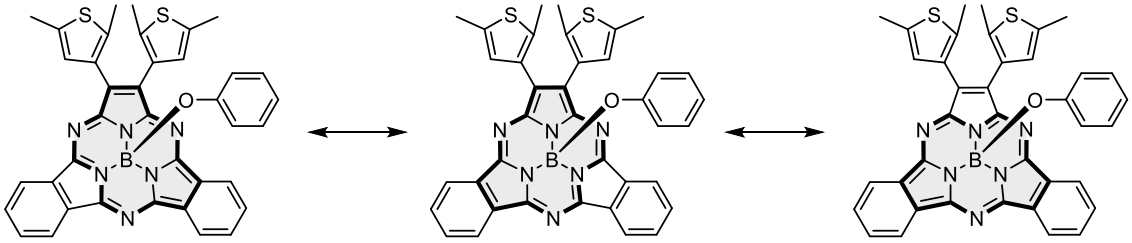

Figure S18. Electron delocalized pathway of **SubPc-DE$_1$**[S5]

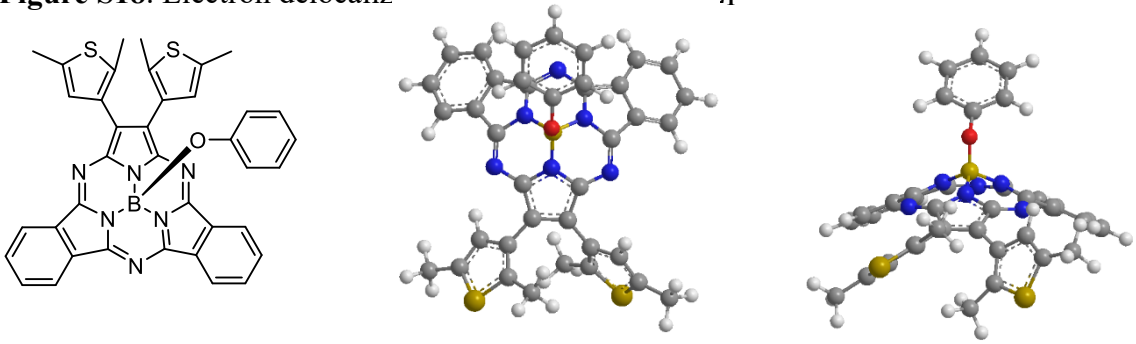

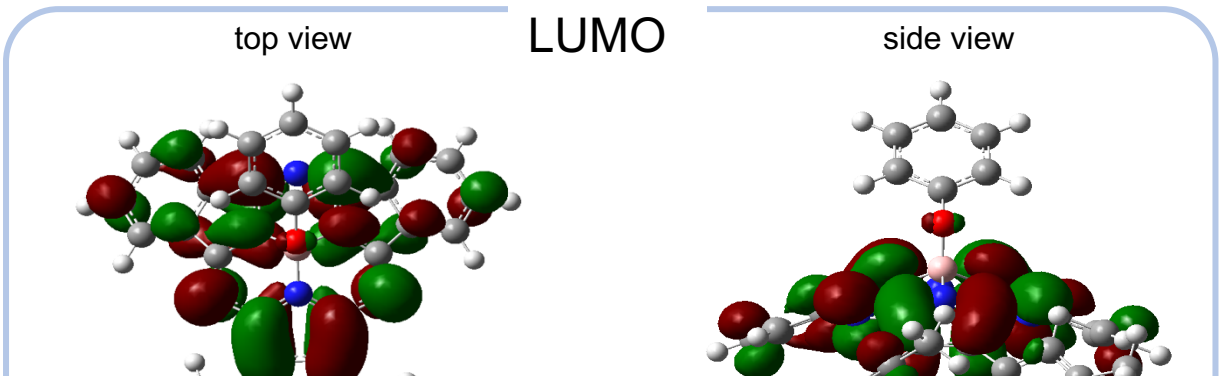

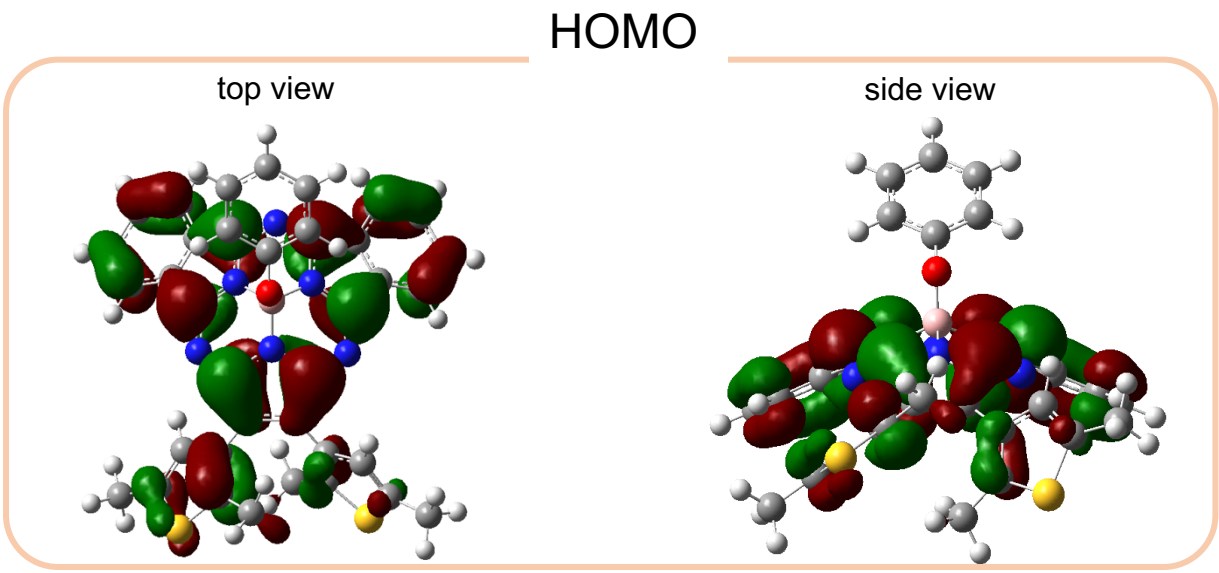

Figure S19 HOMO and LUMO of **SubPc-DE$_1$**. DFT calculation level: B3LYP/6-31+G(d,p)

Transition	f	Main contributions
$S_0 \rightarrow S_1$ (492.77 nm)	0.0320	HOMO - 1 → LUMO (53%) HOMO → LUMO (15%) HOMO → LUMO + 1 (1%)

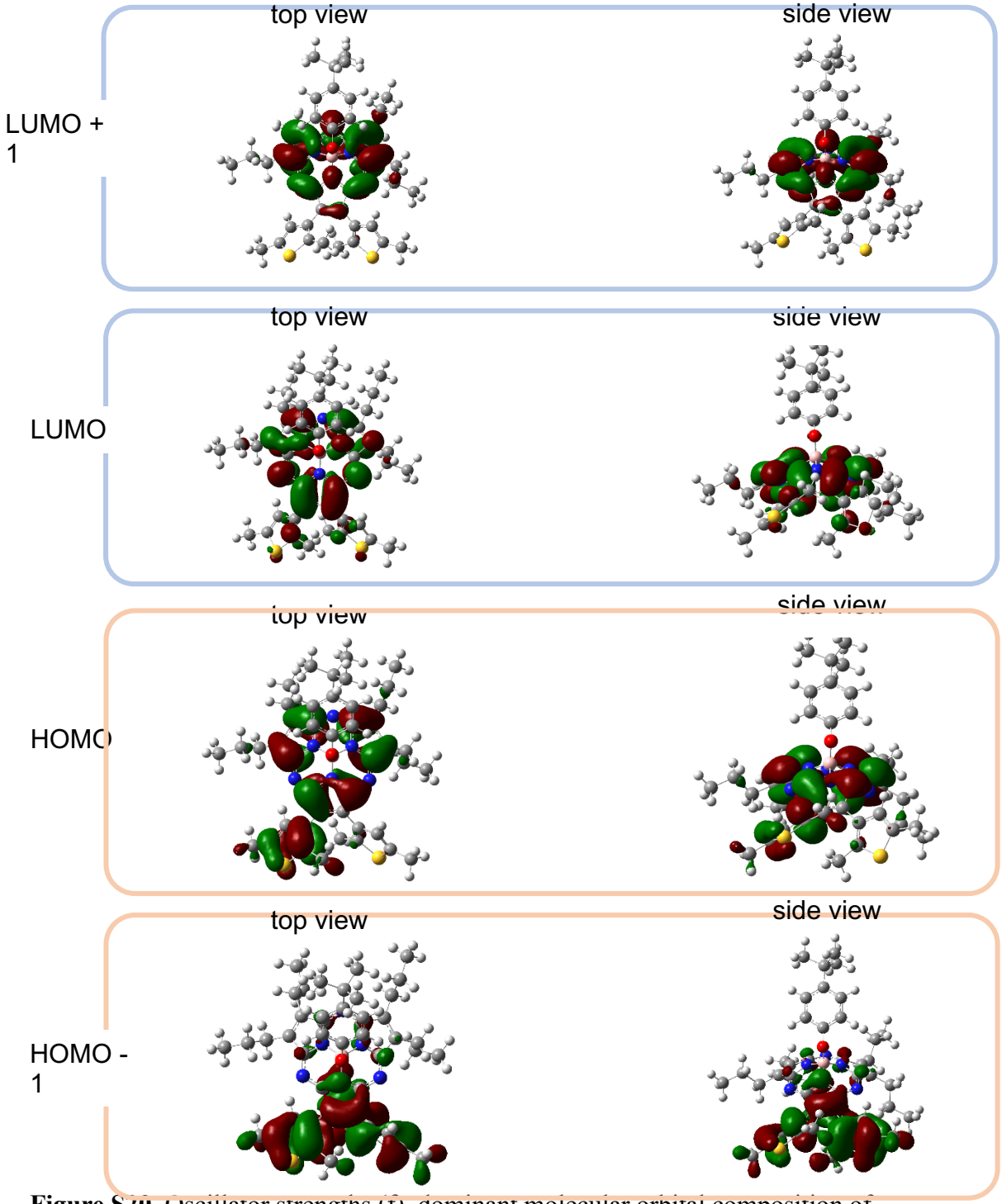

Figure S20. Oscillator strengths (f), dominant molecular orbital composition of $S_0 \rightarrow S_1$ transition and HOMO + 1, HOMO, LUMO, LUMO - 1 for **SubPc-DE$_1$-^{n}Pr**. DFT calculation level: B3LYP/6-31+G(d,p)

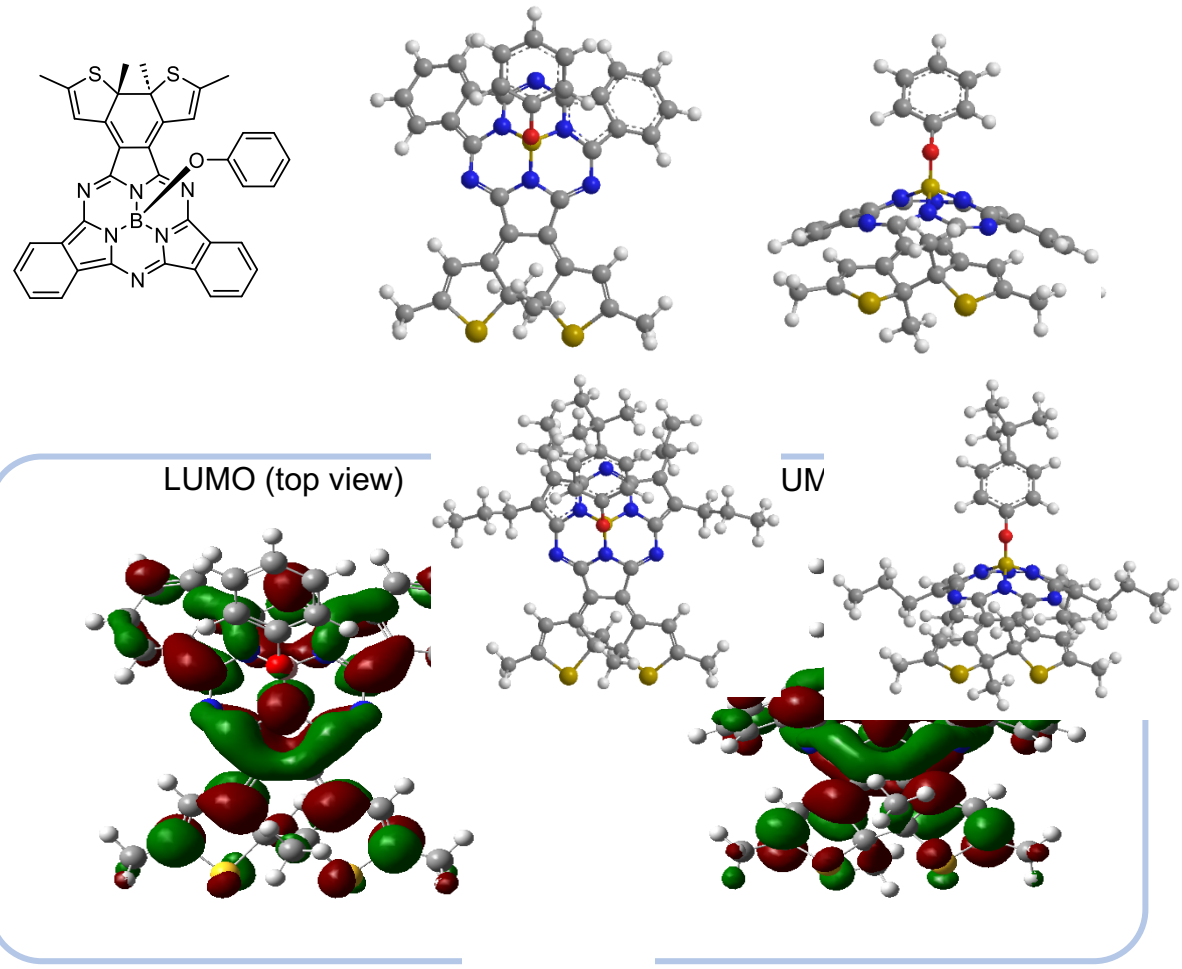

Figure S21. HOMO, LUMO of **SubPc-DE$_1$** (closed form). DFT calculation level: B3LYP/6-31+G(d,p)

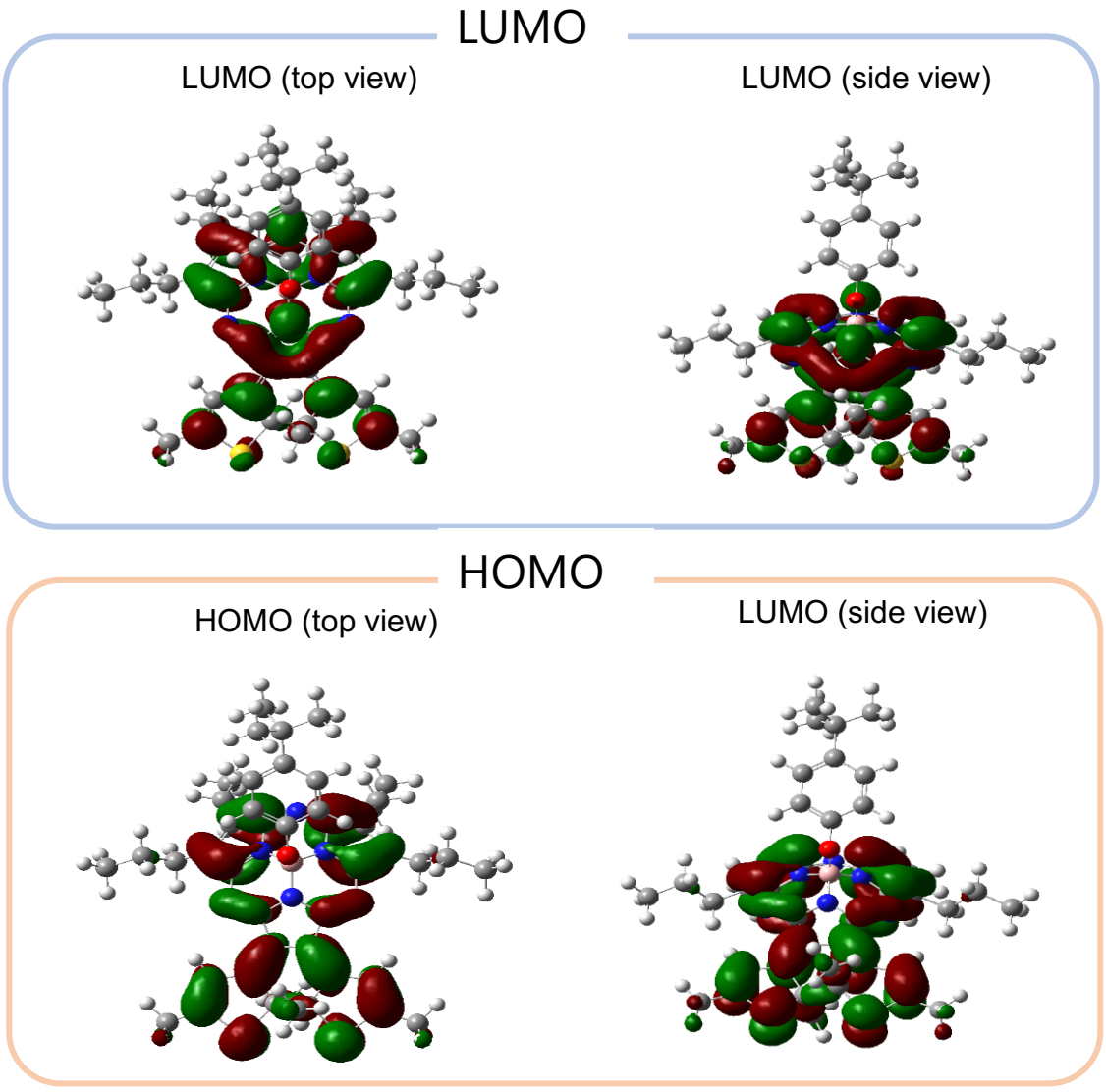

Figure S22. HOMO and LUMO of **SubPz-DE$_1$-^{n}Pr** (closed form). DFT calculation level: B3LYP/6-31+G(d,p)

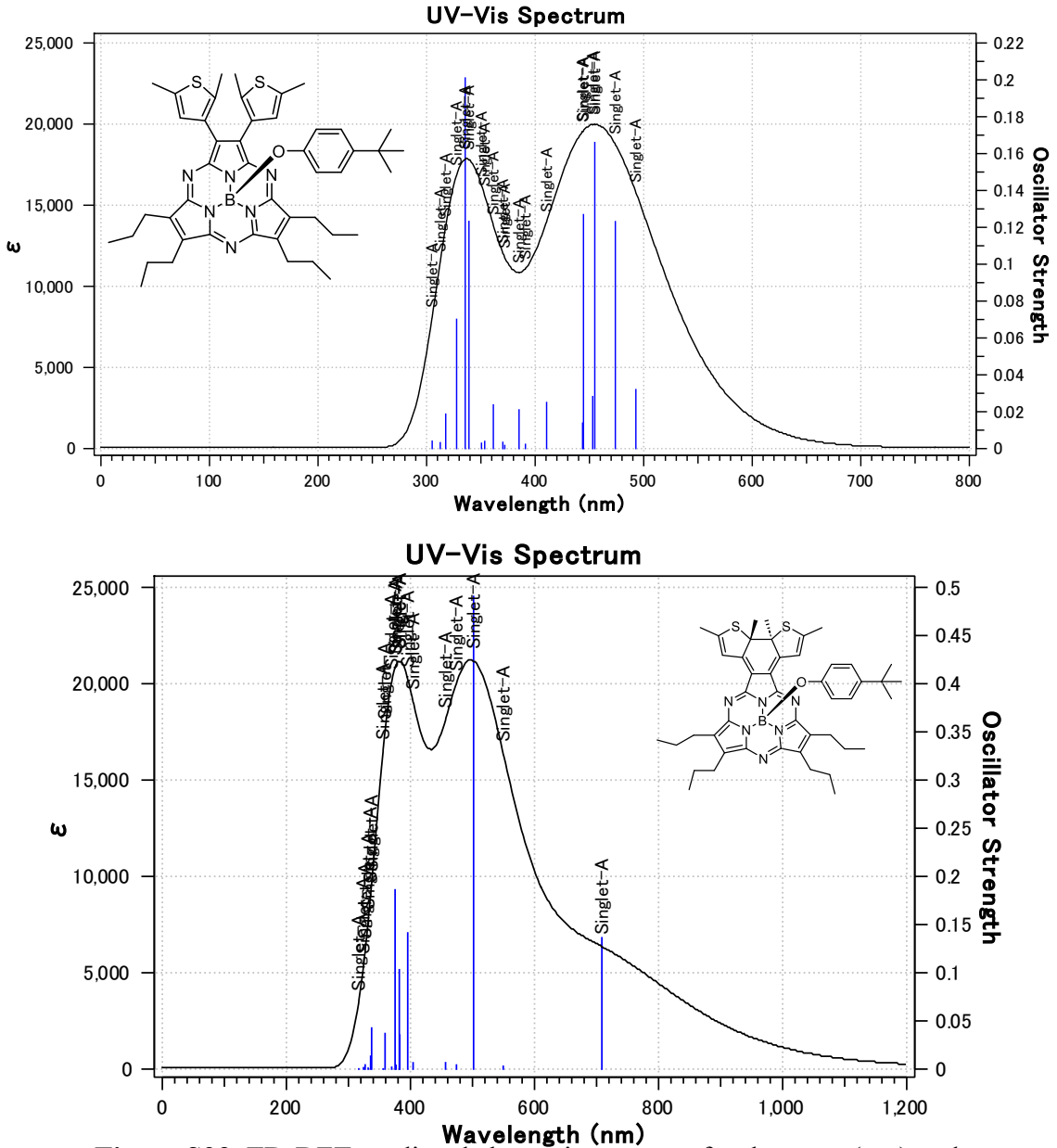

Figure S23. TD-DFT predicted absorption spectra for the open (top) and closed (bottom) **SubPz-DE$_1$-^{n}Pr**. DFT calculation level: B3LYP/6-31+G(d,p)

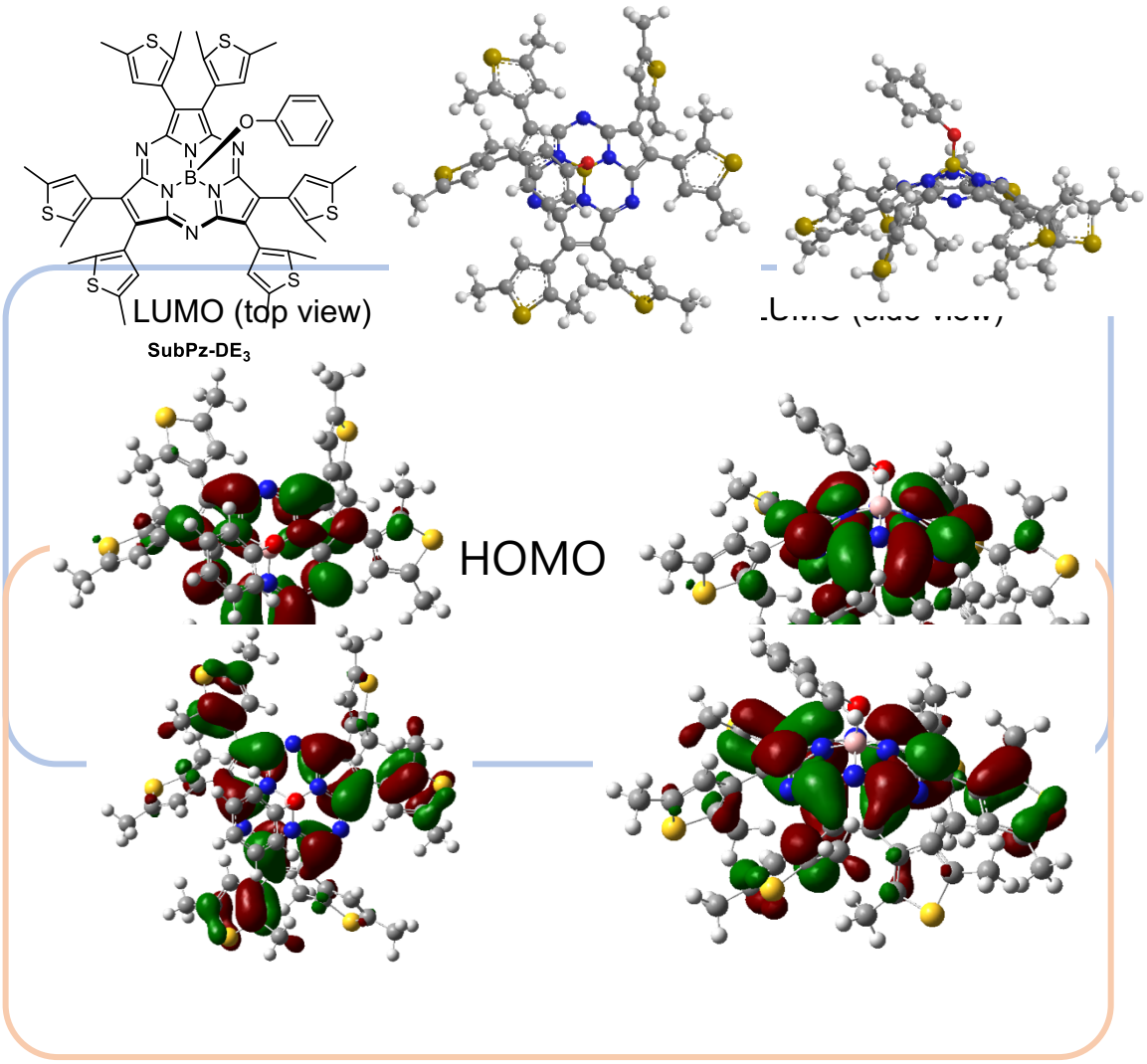

Figure S24. HOMO and LUMO of **SubPz-DE$_3$**. DFT calculation level: B3LYP/6-31+G(d,p)

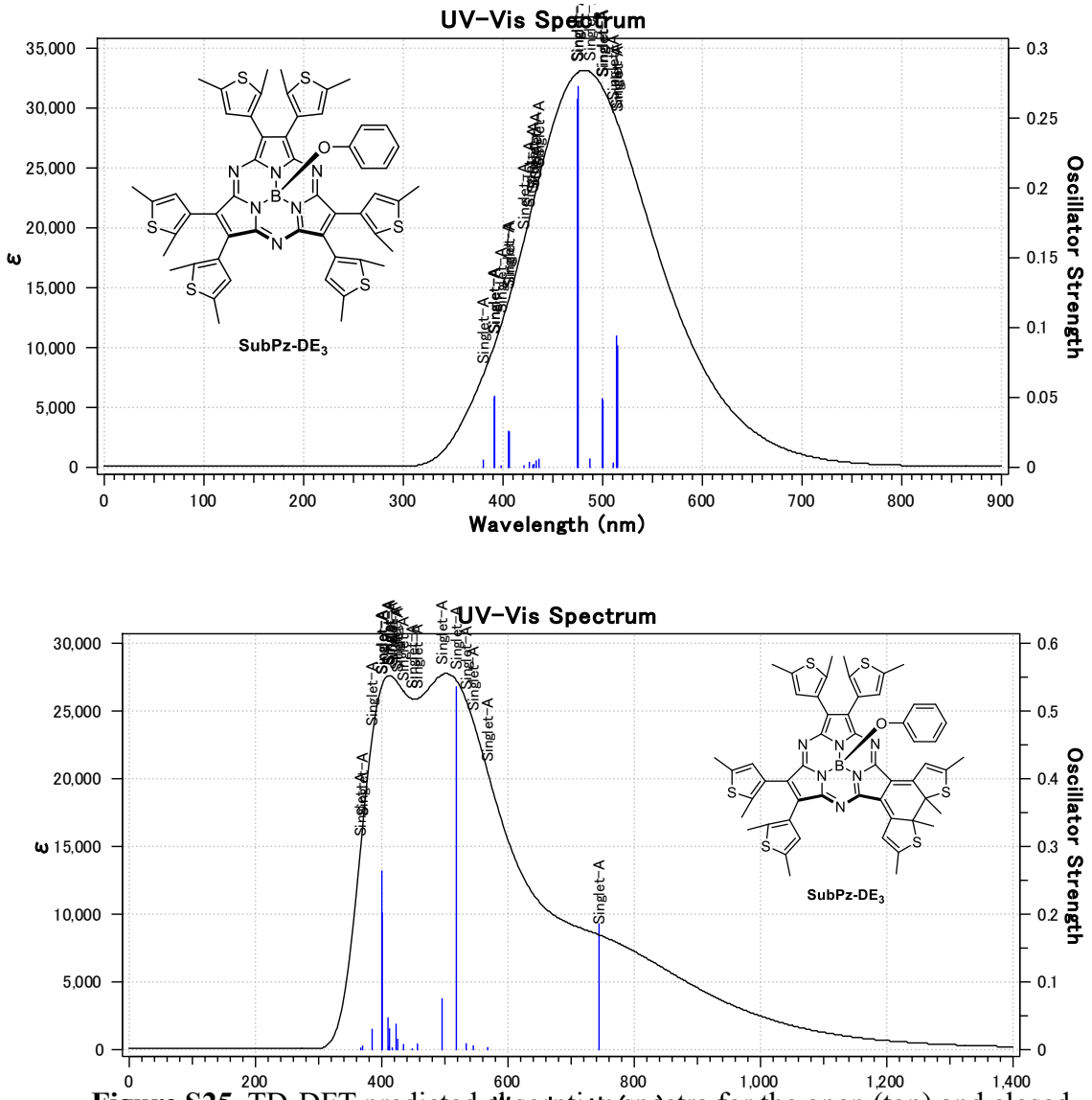

Figure S25. TD-DFT predicted absorption spectra for the open (top) and closed (bottom) **SubPz-DE$_3$**. DFT calculation level: B3LYP/6-31+G(d,p)

References

[S1] T. Yamaguchi, M. Matsuo, M. Irie, *Bull. Chem. Soc. Jpn*. **2005**, *78*, 1145.
[S2] H. Tian, H. Tu, *Adv. Mater*. **2000**, *12*, 1597.
[S3] K. Uchida, Y. Nakayama, M. Irie, *Bull. Chem. Soc. Jpn.* **1990**, *63*, 1311.
[S4] E. Cañizares-Espada, G. Pérez de Bustos, K. Naoda, A. Osuka, T. Torres, M. S. Rodríguez-Morgade, *Org. Lett*. **2024**, *26*, 955.
[S5] Z. Luyang, Q. Dongdong, C. Xue, J. Jianzhuang, *Chin. J. Chem*. **2012**, *30*, 2126.